Journal Pre-proof

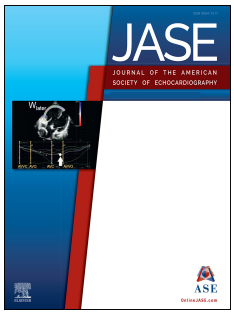

Multimodality Imaging in Evaluating and Guiding Percutaneous Left Atrial Appendage Occlusion

Renuka Jain, MD, Priscilla Wessly, MD, Muhamed Saric, MD, PhD, Karl Richardson, MD, Enrique Garcia-Sayan, MD, Karima Addetia, MD, Lauren Howard, BS, RDCS (AE, PE), RVT, Thomas Finn, BS, Nishath Quader, MD

PII: S0894-7317(25)00397-9

DOI: https://doi.org/10.1016/j.echo.2025.07.009

Reference: YMJE 5622

To appear in: *Journal of the American Society of Echocardiography*

Received Date: 10 April 2025

Revised Date: 18 July 2025

Accepted Date: 20 July 2025

Please cite this article as: Jain R, Wessly P, Saric M, Richardson K, Garcia-Sayan E, Addetia K, Howard L, Finn T, Quader N, Multimodality Imaging in Evaluating and Guiding Percutaneous Left Atrial Appendage Occlusion, *Journal of the American Society of Echocardiography* (2025), doi: https://doi.org/10.1016/j.echo.2025.07.009.

STATE-OF-THE-ART REVIEW

Multimodality Imaging in Evaluating and Guiding Percutaneous Left Atrial Appendage Occlusion

Renuka Jain, MD[a,b], Priscilla Wessly, MD[a], Muhamed Saric, MD, PhD[c], Karl Richardson, MD[d], Enrique Garcia-Sayan, MD[e], Karima Addetia, MD[f], Lauren Howard, BS, RDCS (AE,PE), RVT[a], Thomas Finn, BS[a], Nishath Quader, MD[g]

[a]Aurora Cardiovascular and Thoracic Services, Aurora Sinai/Aurora St. Luke's Medical Centers, 2801 W. Kinnickinnic River Parkway, Ste. 130, Milwaukee, WI 53215 USA
[b]Division of Cardiovascular Medicine, University of Wisconsin School of Medicine and Public Health, Milwaukee Clinical Campus, 2900 W. Oklahoma Avenue, Milwaukee, WI 53215 USA
[c]Leon H. Charney Division of Cardiology, New York University Langone Health, 560 First Avenue, New York, NY 10016 USA
[d]Department of Cardiovascular Medicine, Atrium Health Wake Forest Baptist Medical Center, Medical Center Boulevard, Winston-Salem, NC 27157 USA
[e]Section of Cardiology, Department of Medicine, Texas Heart Institute at Baylor College of Medicine, 6624 Fannin St., Suite 2480, Houston, TX 77030 USA
[f]Section of Cardiology, University of Chicago Heart & Vascular Center, 5842 S. Maryland Ave., Chicago, IL 60637 USA
[g]Division of Cardiovascular Medicine, Washington University in St. Louis, 1 Brookings Drive, St. Louis, MO 63130 USA

Running Title: Multimodality Imaging in LAAO
Word Count: 4,887
Tweet: State of the Art Review on multiple modalities that can be used for all steps in LAAO procedure #echofirst @yesCT @renujain19 @EGarciaSayan @PWesslyMD @nishath_quader

Corresponding author:
Renuka Jain, MD
Aurora Cardiovascular and Thoracic Services
Aurora St. Luke's Medical Center
2801 W. Kinnickinnic River Parkway, Ste. 130
Milwaukee, WI 53215
Email: wi.publishing159@aah.org

Abstract

Left atrial appendage occlusion (LAAO) has emerged as an important intervention for stroke prevention in patients with non-valvular atrial fibrillation (AF) who are unable to tolerate long-term anticoagulation. The development of advanced imaging technologies and techniques, such as 3D echocardiography with multiplanar reconstruction (MPR), multidetector computed tomography (MDCT), 3D intracardiac echocardiography (ICE), 3D printing, and simulation, has revolutionized pre-procedural planning, intra-procedural guidance, and post-procedural surveillance, ensuring improved precision and outcomes. Transesophageal echocardiography (TEE) remains a foundational imaging modality for assessing LAA morphology, excluding thrombi, and obtaining accurate measurements for device sizing. Recent advances in 3D TEE and MPR techniques enable enhanced visualization of complex LAA anatomies, improving device selection and procedural planning. Multidetector computed tomography has a growing role, offering high-resolution 3D reconstructions for detailed anatomical assessment. Additionally, its applications in 3D printing and virtual device simulation provide patient-specific insights, facilitating optimal device sizing and improving procedural efficiency. Intra-procedurally, 3D ICE has gained traction as a valuable alternative to TEE. With its real-time imaging capabilities and high spatial resolution, 3D ICE allows precise guidance during transseptal puncture and device deployment while reducing the need for general anesthesia. Post-procedurally, both TEE and MDCT play critical roles in assessing device stability and identifying complications such as device-related thrombus and peri-device leak. This review highlights the evolving role of multimodality imaging in LAAO, including innovations such as 3D ICE, 3D printing, and simulation. It also reviews recent literature to establish state-of-the-art

imaging practices, providing a comprehensive discussion of imaging applications across pre-, intra-, and post-procedural phases to optimize outcomes and minimize complications in LAAO.

Keywords: echocardiography, left atrial appendage, left atrial appendage occlusion, multimodality imaging, transesophageal echocardiography

Abbreviations

3DP = 3D printing

AF = atrial fibrillation

CT = computed tomography

DRT = device-related thrombus

FDA = US Food and Drug Administration

HAT = hypoattenuated thickening

ICE = intracardiac echocardiography

LAA = Left atrial appendage

LAAO = Left atrial appendage occlude/occlusion

LUPV = left upper pulmonary vein

MDCT = multidetector CT

MPR = multiplanar reconstruction

PDL = peri-device leak

TEE = transesophageal echocardiogram/echocardiography

INTRODUCTION

Atrial fibrillation (AF) affects more than 33 million people worldwide and is the second-leading cause of stroke, resulting in significant clinical morbidity.[1,2] Echocardiographic studies show that more than 90% of thrombi in non-valvular AF form in the left atrial appendage (LAA).[3] Anticoagulation therapy significantly reduces the risk of ischemic stroke and all-cause mortality. However, more than 50% of eligible patients either discontinue or avoid anticoagulants because of bleeding concerns, side effects, or noncompliance.[4] Alternative strategies for stroke prevention are therefore needed. The concept of LAA exclusion dates to 1949 when John L. Madden performed surgical resection to prevent recurrent arterial thrombi.[5] Surgical LAA exclusion strategies offered a viable option for patients unable to tolerate long-term anticoagulation, but evidence of efficacy was limited.

The PROTECT AF (WATCHMAN Left Atrial Appendage System for Embolic Protection in Patients With Atrial Fibrillation)[6] and PREVAIL (WATCHMAN LAA Closure Device in Patients With Atrial Fibrillation Versus Long Term Warfarin Therapy)[7,8] trials demonstrated that percutaneous LAA occlusion (LAAO) device implantation was non-inferior to warfarin for stroke prevention in non-valvular AF. The approval of the first plug-like transcatheter LAAO device (with a single occlusive mechanism) in 2015 marked a milestone in LAAO therapy. In 2021, the US Food and Drug Administration (FDA) approved a second device, a disk-and-lobe system (a dual occlusive mechanism) that was shown in the Amulet IDE (Amplatzer Amulet LAA Occluder) trial[9] to have non-inferior efficacy, further expanding the available stroke prevention options (Figure 1).

LAA size, shape, and relationship with surrounding structures vary significantly between patients, and these anatomical differences impact the success of LAAO procedures.

Transesophageal echocardiography (TEE) has traditionally been used to evaluate LAA morphology, guide LAAO procedures, and monitor post-implantation outcomes. Recently, real-time 3D intracardiac echocardiography (ICE) has gained popularity for LAAO guidance, offering imaging with high spatial and temporal resolution. Multidetector cardiac computed tomography (MDCT) has emerged as a key tool in pre-procedural planning, providing detailed 3D reconstructions that allow for accurate device sizing and visualization of complex LAA anatomy.

This review aims to explore the role of multimodality imaging in pre-procedural evaluation, intra-procedural guidance, and post-procedural follow-up in percutaneous LAAO (Central Illustration). It also addresses the use of imaging in assessing device-related complications during follow-up and highlights the latest advances in and future directions of this evolving field.

PRE-PROCEDURAL EVALUATION

Transesophageal Echocardiography

Transesophageal echocardiography served as the primary imaging modality in pivotal clinical trials.[7,9,10] Accurate image acquisition is operator-dependent, and adherence to a comprehensive protocol is crucial for reliable measurements and conclusions.[11] The goals of TEE in the context of screening and planning for percutaneous LAAO procedures are to determine LAA morphology, exclude LAA thrombus, and perform measurements of the landing zone, thereby facilitating optimal device selection and sizing. A thorough TEE examination is recommended to evaluate left ventricular size and function, aortic plaque, aortic or mitral valve pathology (especially mitral stenosis), pericardial effusion, intracardiac masses, and the atrial septum. Baseline TEE should particularly evaluate for mitral stenosis, a marker for valvular AF, to ensure

eligibility by identifying patients excluded from trials like PROTECT AF and PREVAIL. The role of percutaneous LAAO for valvular AF is currently unknown, with clinical equipoise persisting regarding its efficacy.[6-8] Atrial septal defects, atrial septal aneurysms, and existing atrial occluder devices may all present challenges or contraindications to the procedure.

On 2D TEE, the LAA is typically imaged at 4 omniplane angles in 45-degree intervals (0º, 45º, 90º, 135º) with and without color Doppler. Color-flow Doppler imaging can reveal areas with decreased or absent color flow within the appendage, which is highly suggestive of thrombi. Dedicated and zoomed images are recommended for improved accuracy. The shape of the LAA is determined by the number and location of appendage lobes. A "windsock" morphology is characterized by a prominent single lobe, a "cactus" morphology by 2 roughly equal lobes, a "chicken wing" morphology by a lobe that arises at an acute angle from the LAA ostium (anterior or posterior to the ostium), and a "cauliflower/broccoli" morphology by multiple lobes and variable depth (Figure 2). These morphologies influence device selection and success. Although 2D imaging can be used to determine LAA morphology, 3D echocardiography with a zoom volume acquisition of the LAA provides a more accurate depiction of the shape, number, and location of lobes. New 3D rendering algorithms, such as light-source manipulation and transillumination technologies, can enhance visualization of the LAA morphology and allow orientation of the images to resemble fluoroscopic views (Figure 2).[12,13] Both the 3D LAA multiview (LAAM) and tilt up and turn left (TUPLE) maneuvers are algorithms developed in step-wise fashion to assess LAA morphology in 3D (Figures 3 and 4).

For the plug-like LAAO device, key measurements include the landing zone, with the ostium width measured as the distance from the left circumflex coronary artery extending radially to the opposing limbus, often approximating 2 cm from the tip of the limbus (Figure

5A). The maximum width of the anticipated landing zone is determined and used for device sizing according to the manufacturer's recommendations. The measured landing zone must be between 14 mm and 36 mm to accommodate the WATCHMAN FLX/PRO device (Boston Scientific, Marlborough, Mass). The LAA depth is measured from the center of the anticipated landing zone to the LAA apex and should be more than 50% of the labeled device diameter.

For the disk-and-lobe LAAO device, the LAA orifice should be measured to ensure it is smaller than the anticipated diameter of the device disk. The anticipated landing zone of the device lobe is measured 10-12 mm distal to the LAA orifice, defined as the plane extending from the tip of the limbus to a location just proximal to the left circumflex coronary artery. The measured landing zone must be between 11 mm and 31 mm and is used for device sizing, as determined by the device manufacturer. The LAA depth is measured from the center of the LAA orifice ostium and then perpendicular to the length of the LAA orifice. Figure 5B demonstrates the 2D LAA sizing measurements for the Amplatzer Amulet device (Abbott Cardiovascular, Abbott Park, IL).

For both device styles, the manufacturers' recommendations and instructions for use suggest 2D measurements at the 4 omniplane angles. However, 2D measurements of a 3D orifice can lead to uncertainty about the exact plane of measurement and potential underestimation if not centered in the orifice. Three-dimensional echocardiography with multiplanar reconstruction (MPR) can provide precise measurements of the orifice and landing zone, ensuring all measurements are performed in the same plane. This approach also allows visualization of the deepest lobe and has been shown to lead to more accurate device sizing (Figure 6).[14,15]

Multidetector Cardiac Computed Tomography

Multidetector cardiac computed tomography has a growing role in pre-procedural planning for LAAO procedures owing to its excellent spatial resolution and ability to generate precise, high-quality 3D measurements. It can replicate the key aspects of TEE in evaluating LAA morphology, maximum ostium diameter, and depth for device selection and eligibility (Central Illustration). Increasingly, MDCT is recognized as a primary imaging modality for LAAO planning, often reducing the need for pre-procedural TEE. In many centers, patients may undergo TEE only at the time of device implantation, whereas in others, LAAO may be performed using ICE-guided deployment. Filby et al. demonstrated that pre-procedural planning guided by cardiac computed tomography (CT), in combination with ICE-guided device deployment, achieved a 97.2% accuracy in device sizing and 100% procedural success in 71 patients, supporting the feasibility of non-TEE workflows with comparable outcomes.[16] This shift underscores MDCT's ability to provide comprehensive anatomical and functional data, facilitating efficient procedural planning and enabling same-day discharge strategies in select cases.

Standardized MDCT acquisition protocols for evaluating the LAA have been established using a 2-phase scan approach and may vary based on the scanner system used.[17] The first phase consists of a prospective or retrospective electrocardiographically gated scan acquisition during systole (typically 30-60% of the R-R interval) that provides high-resolution images for a detailed assessment of LAA morphology and size. This is followed by a delayed acquisition, performed 30-180 seconds later, to reliably exclude the presence of an LAA thrombus in patients who may have delayed opacification of the LAA. A meta-analysis of 19 studies showed that MDCT has a high negative predictive value (96-100%) for detecting LAA thrombi. Delaying imaging by at

least 30 seconds after the contrast bolus is administered is mandatory and improves the mean positive predictive value from 41% to 92% or greater.[18]

Several image processing workstations (Vitrea Workstation, Aquarius Workstation, Brilliance Workstation, and 3mensio software among others) use MPR (a volume-rendering process used to produce 2D planes from 3D datasets) to reassemble and manually manipulate images of the LAA and surrounding structures. By rotating the axial view 30º right anterior and the sagittal view 10º cranial, an oblique angle is reached to view the LAA orifice en face. Here, the maximum LAA depth, ostium diameter, and landing zone diameter are measured (Figure 7A and 7B).

The 3D data provided by MDCT images enable advanced applications in procedural planning. For example, advanced software applications can assist with planning the optimal transseptal puncture location and C-arm position (Figure 7C) and display a virtual device in a 3D rendering (Figure 7D). Multidetector cardiac computed tomography datasets can also be used for 3D printing (3DP), generating models to visualize the LAAO implantation and transseptal puncture *in vitro.* Studies have demonstrated that 3DP improves device size accuracy compared to CT and TEE alone and can identify optimal transseptal puncture locations.[19-21] Additionally, artificial intelligence-enabled MDCT anatomical analyses and computer simulations can improve outcomes. De Backer *et al.* demonstrated that using MDCT with FEops HEARTguide simulation technology (FEops NV, Ghent, Belgium) significantly improved procedural efficiency over standard practices, reducing total procedure times (55.2±24.7 vs 45.1±18.3 min, p=0.01) and radiation times (17.6±11.4 vs 12.5±6.8 min, p<0.001) and increasing rates of single-device, single-deployment (58.0% vs 29.9%, p<0.001).[22]

Comparison of Imaging Modalities

The first studies comparing imaging modalities for LAAO emerged in 2016. Wang *et al.* (n=53) concluded that measurement by both 2D and 3D TEE significantly undersized the LAA landing zone ($p \leq 0.0001$).[23] Saw *et al.* (n=50) highlighted that CT and TEE imaging modalities were not interchangeable, with MDCT measurements for both plug-like and disk-and-lobe devices being larger on CT than TEE.[24] In one small study, the use of MDCT-derived LAA measurements significantly improved device size accuracy, achieving 92% accuracy (11/12) compared to 27% accuracy (3/11) with TEE (p=0.01). This accuracy translated into enhanced procedural efficiency with reduced procedural time (55±17 vs 73±24 min, p=0.05), fewer devices required per procedure (1.3±0.7 vs 2.5±1.2 devices, p=0.01), and fewer delivery sheaths (1 per case vs 1.7±0.7 sheaths, p=0.01) used.[25] A meta-analysis by Sattar *et al.* found that despite LAA orifice measurements that were significantly larger on MDCT imaging than on TEE imaging, there was no significant difference in the number of devices used or in the odds of correct device sizing when only MDCT and TEE measurements were compared. However, when studies utilizing MDCT-based 3D modeling were included, MDCT demonstrated significantly higher odds of correct device sizing compared to TEE (OR 1.64; 95% CI 1.05-2.56, p=0.03). Additionally, MDCT imaging resulted in significantly reduced fluoroscopy time compared to TEE.[26] These findings underscore the utility of pre-procedural MDCT imaging in improving procedural efficiency and outcomes in LAAO procedures.

Favorable and Unfavorable Anatomies for LAAO

The success of LAAO procedures depends on the anatomical characteristics of the LAA, which must be evaluated to select the appropriate device and optimize outcomes. Favorable and unfavorable morphologies can be described for plug-like devices and disk-and-lobe devices (Table 1).

Plug-like devices

Favorable Anatomies: Windsock- and cactus-shaped LAAs that have an orifice measuring 14-36 mm and a minimum depth of approximately 50% of the device width allow higher compression and better success rates (Figure 8A).

Unfavorable Anatomies: The chicken wing and cauliflower/broccoli morphologies, or orifices <14 mm or >36 mm, pose challenges with lower compression and success rates. Additionally, extremely elliptical LAA orifice or high eccentricity index (maximum diameter/minimum diameter ≥1.5) pose significant challenges, increasing the risk of residual leaks even with oversized devices. Insufficient depth (<50% of device length) or large mid-cavitary pectinates may lead to a large shoulder with incomplete sealing, residual leaks, or device embolization (Figure 8B).[27]

Disk-and-Lobe Devices

Favorable Anatomies: These devices perform well in LAAs with an orifice diameter of 11-31 mm and depth of ≥10-12 mm. They are ideal for anatomies with oval-shaped landing zones, large mid-cavitary pectinates, and secondary lobes (<1 cm depth). Disk-and-lobe devices are positioned more proximally than plug-like devices, allowing for adequate LAA closure in these anatomies. For LAAs that have a very short neck and sharp acute bends, such as in the chicken wing morphology, the implantation and complete closure rates are very high (98-99%) owing to the dual-closure design and ability to anchor on the proximal part of the LAA.[28]

Unfavorable Anatomies: Very small (<11 mm) or very large (>31 mm) landing zone diameters and insufficient depth (<10 mm) compromise device stability and sealing.

Accurate pre-procedural imaging and detailed anatomical assessment are essential for choosing the most suitable device, enhancing procedural success, and optimizing long-term patient outcomes.

INTRA-PROCEDURAL EVALUATION

Transesophageal Echocardiography

Intra-procedural TEE is the primary imaging modality for LAAO and was used in all the LAAO clinical trials. Intra-procedural TEE is performed to confirm LAA measurements and to rule out LAA thrombi. When spontaneous echocardiographic contrast (SEC) or sludge is present in the left atrium or LAA, differentiating a thrombus from the sludge/SEC becomes challenging, necessitating additional TEE enhancements.[29] Guidelines from the American Society of Echocardiography recommend the consideration of ultrasound enhancing agents during TEE for the assessment of LAA thrombus when there is SEC or poor visualization (COR IIa, LOE B-NR).[30] Ultrasound enhancing agents improve thrombus identification and differentiation of SEC degrees, with studies demonstrating increased interpretative confidence, reader agreement, and prevention of procedure cancellations.[31] Dobutamine and isoproterenol, both positive inotropic agents, have been shown to resolve LAA SEC and significantly increase peak LAA velocity.[32,33] There were no strokes, systemic embolisms, or device-related thrombi reported on follow-up with the use of dobutamine or isoprotenerol.[34]

Disk-and-lobe and plug-like devices both require transfemoral venous access and have several common steps (Figure 9, Videos 1-4). Once femoral access is obtained, TEE imaging is utilized to guide the transseptal puncture. A delivery catheter and needle are advanced to the interatrial septum. Both 2D or 3D TEE views can be used to visualize the inferior, superior, anterior, and posterior portions of the interatrial septum. The choice of transseptal puncture site

is guided by the LAA's anatomy, with an inferoposterior puncture recommended in 75-80% of cases to ensure coaxial alignment between the delivery sheath and the proximal LAA central axis. However, an inferior but more central or anterior transseptal puncture is preferred in 20-25% of cases, particularly in those with reverse chicken wing LAA morphology or posterior bending of the proximal LAA.[35,36] As most LAAs are anteriorly directed, a posterior puncture is desirable in most cases. The 90° TEE view aids in gauging LAA direction, complemented by pre-procedural cardiac CT analysis. Once the delivery sheath has crossed the interatrial septum, it is advanced into the left atrium and the distal end of the sheath is positioned near the LAA ostium.

The plug-like device is initially unsheathed to form a ball, which can be manipulated in the LAA to achieve an ideal trajectory and then be fully deployed. Figure 10 and Videos 5-8 outline the steps for deployment of a plug-like device. The location of the circumflex artery in relation to the ostium should be noted, with the plane of maximal device diameter positioned at or just distal to the ostium, ensuring that any protrusion or "shoulder" (if present) does not exceed 40-50% of the device depth. For plug-like devices, the anatomical orifice is defined by a line connecting the circumflex artery and a point 10-20 mm inside the LAA from the left upper pulmonary vein ridge, described as the beginning of the trabeculated LAA, and is intended to be covered by the device. Compression is measured from shoulder to shoulder with the central metallic "threaded insert" visible on the left atrial side and is assessed at 0º, 45º, 90º, and 135º. A "tug test" is performed under TEE and/or fluoroscopic visualization to confirm stability, ensuring that the device returns to its original position. Once stability is confirmed, peri-device leaks (PDLs) should be carefully assessed using multiplanar imaging at 0º, 45º, 90º, and 135º

with color Doppler and the Nyquist limit set at 20-30 cm/sec to detect low-velocity flows. Any significant PDL should be avoided, and the device recaptured and redeployed if needed.

For disk-and-lobe devices, the steps for deployment are outlined in Figures 11 and 12 (Videos 9-17). The device lobe should be two-thirds deeper than the circumflex artery to ensure proper sealing and compression. The lobe is initially unsheathed to form a ball. This ball can be manipulated into the LAA. Once the position and trajectory are optimized, this lobe is fully deployed, initially appearing as a triangle shape before full deployment. The disk is deployed subsequently, ensuring that it covers the anatomic ostium of the LAA and does not impinge upon the left superior pulmonary vein, which is separated from the LAA by a ridge.

Once the device is deployed, each type of device has a protocol for the assessment of position, stability, compression, and seal (Figure 13 for plug-like device, Figure 14 for disk-and-lobe device). A color Doppler "twinkling" artifact might be noted over the proximal surface of nitinol-based PTFE-covered devices. This artifact arises from ultrasound interactions with the strongly reflective surface and appears as a red-blue shimmer, mimicking flow, and should not be misinterpreted as PDL. This can be distinguished by its diffuse pattern, a lack of continuity across the device, and the absence of a corresponding signal on spectral Doppler. If the release criteria are met, the device is released and the guide catheter is withdrawn from the left atrium; color Doppler and 2D TEE are then used to assess the size of the atrial septal defect and flow direction. A 3D view of the LAAO device is obtained to confirm its proximity to the mitral annulus and surrounding structures. A final assessment of pericardial effusion is performed prior to removing the TEE transducer.

Micro- and Mini-TEE

Micro- and mini-TEE probes, originally designed for pediatric diagnostic imaging, are emerging as alternatives to standard TEE probes for LAAO guidance, particularly in frail patients or those for whom general anesthesia is unsuitable. These smaller-diameter probes (with 32 and 48 imaging elements, respectively, vs. >2,500 in standard TEE) enable the use of conscious sedation, thereby reducing anesthesia-related risks and logistical challenges. In a recent study, micro- and mini-TEE provided adequate imaging in 99.3% of LAAO cases, with only 0.7% of cases requiring conversion to standard TEE, supporting the feasibility of these probes for this procedure.[37] However, limitations include reduced image quality as a result of fewer imaging elements, challenges in maintaining esophageal wall contact because of their smaller flexible design, and diminished far-field resolution in patients with large atria owing to higher probe frequencies. Despite these challenges, micro- and mini-TEE are particularly appealing to operators who seek minimalist LAAO approaches, offering a balance between TEE's familiarity and ICE's reduced anesthesia requirements, with the added benefit of lower gastrointestinal complication risk compared to standard TEE.

Intracardiac Echocardiography

Intracardiac echocardiography has gained popularity in guiding LAAO procedures, particularly with the advent of 3D real-time ICE imaging. The procedure follows the same steps as with TEE. The ICE transducer is inserted into the right atrium and utilized to cross the interatrial septum. Imaging in 3D is essential to evaluate anterior-posterior and superior-inferior portions of the septum. Once the septum has been crossed, the ICE transducer is advanced through the puncture site into the left atrium. With the ICE transducer in the left atrium, the absence of any LAA thrombi is confirmed and measurements of the LAA ostium and depth are obtained, preferably from the 3D dataset. Intracardiac echocardiographic views should be optimized to create 3

"TEE-like" views (Figure 15) to optimize the position and trajectory of the device. The mid left atrial view resembles the 45° TEE view and is used during LAA device deployment. The left superior pulmonary vein view resembles the 90º TEE view and is used to assess maximum LAA depth. The supramitral view is akin to the 135º (high angle) TEE view, which is critical to assess device position, seal, and compression (Figure 15).

At this stage, it is unclear whether ICE-guided LAAO is a more cost-efficient method for LAA procedures and whether it is associated with better outcomes and shorter procedure times. In some cases, ICE could potentially eliminate the need for general anesthesia.[38] In a study by Berti *et al.,* ICE guided LAAO with a procedural success rate of 93% and there was a significant correlation in measurements for device sizing between ICE and angiography.[39] A recent meta-analysis demonstrated that ICE provides comparable efficacy and safety, with reduced use of contrast and shortened fluoroscopy and procedure times.[40] However, a multicenter study showed that, although ICE-guided LAAO achieved high procedural success rates, TEE-guided procedures were associated with shorter procedure and fluoroscopy times.[41] The potential for ICE-guided LAAO without fluoroscopy is a significant advancement, with studies demonstrating feasibility for sizing, deployment, and PDL assessment without contrast. Successful cases with plug-like devices achieved zero fluoroscopy, with comparable procedural times to the conventional method.[42,43] This approach reduces radiation risks and eliminates the need for general anesthesia, enhancing patient comfort, although it involves a larger transseptal puncture and a learning curve. Further, each modality comes with unique complications: whereas TEE has been associated with higher gastrointestinal complications, ICE has been associated with increased peripheral vascular and renal complications.[44] Additional considerations include the cost of the ICE catheter, the learning curve for operators, and current reimbursement challenges.

Complications of LAAO Procedures

Intra-procedural complication rates are low with both types of devices. Pericardial effusion/tamponade can be a complication of transseptal puncture. Other complications include device-related embolization and procedure-related ischemic stroke.[10] The disk-and-lobe device has been found to have a slightly higher risk of pericardial tamponade or major bleeding.[45] Table 2 details the complications of LAAO procedures.[7,10,46-48] Importantly, the rate of complications decreases with operator experience. Intraprocedural imaging with TEE or ICE is key for both device placement and the monitoring of these complications.

POST-PROCEDURAL EVALUATION

Post-Procedural Imaging Protocols

The 2023 consensus statement by the Society for Cardiovascular Angiography and Interventions and the Heart Rhythm Society recommends follow-up imaging with TEE or MDCT between 45 and 90 days post-LAAO to assess device sealing. A second follow-up at 1 year should be considered if there is concern about device-related thrombus (DRT) or PDL. If DRT was detected, repeat imaging using TEE or MDCT every 45 to 90 days is recommended.[36]

Nestelberger *et al.* recommended similar surveillance strategies: TEE or MDCT 6-12 weeks post-LAAO and another routine TEE or MDCT at 12 months if the patient is at high risk for DRT. A key difference from the 2023 consensus statement is their recommendation for routine transthoracic echocardiography at 12 months to assess atrial sizes, ventricular and valvular function, and potential late device embolization. They also favor MDCT for surveillance at 6-12 weeks owing to its higher spatial resolution, sensitivity in the detection of PDL, and non-invasive and non-fasting nature. However, they acknowledged the radiation and subsequent risk

associated with CT utilization and emphasized that TEE remains a valuable modality for LAAO follow-up imaging.[49]

Imaging of DRT

DRT is one of the more troublesome findings on follow-up imaging, with the reported incidence ranging from 1.7% to 7%.[50,51] Device-related thrombi vary widely in size,[52] and their clinical impact is worrisome (Table 3). Few trials were reassuring,[9,56] and the majority of data point to a 3.5-4 times higher risk of ischemic events in patients with DRT than in those without DRT.[53,54,57] The timing of the occurrence of DRT is somewhat unpredictable: 58% of DRT cases were diagnosed after 3 months in a meta-analysis and 18-36% of DRT were seen after 6 months in large registry studies, well after the presumed device endothelialization period.[52,53,57]

Predicting the occurrence of DRT requires consideration of several clinical, imaging, and procedural risk factors. The most commonly cited clinical risk factors include advanced age,[50,58] prior embolic events,[54,58] higher CHA_2DS_2-VASc score,[59] and permanent AF.[50,52] Pre-implant imaging findings that are associated with subsequent DRT include larger LAA orifice width, larger left atrial size, lower left ventricular ejection fraction, lower peak emptying velocity, and SEC.[54,57,60-62] Interestingly, neither LAA morphology nor anticoagulation regimen predicted DRT occurrence.[53,57]

Deep implantation has emerged as the strongest procedural risk factor for DRT.[57,59,63] Similarly, one study correlated the uncovered area—defined as the triangular area between the tip of the ridge, the surface of the device, and the mitral annulus—with the risk of DRT.[63] This cul-de-sac between the exposed ridge and the face of the device has been termed a "neo-appendage"[63,64] and has been shown to increase turbulence. Additionally, off-axis deployment

and residual PDL have also been associated with DRT risk.[57,65] Finally, the literature suggests that DRT can also occur centrally, adherent to the central screw of the device (Figure 16).[52,57]

TEE has historically been the standard post-deployment surveillance imaging modality.[66] The expert consensus definition of DRT by TEE is an echo density that is not explained by artifact, not typical of healing, visible in multiple planes, in contact with the device, and independently mobile.[67,68] The rise in MDCT imaging has yielded markedly high rates of hypo-attenuated thickening (HAT), which resembles thrombus but has an uncertain clinical significance. Recent studies show HAT in a significant majority of cases, leading to classification of HAT into low-grade (smooth, covering the entire device, and continuous with the left atrial wall) and high-grade (not continuous with the left atrial wall, having irregular borders or being pedunculated).[69,70] High-grade HAT, which occurs far less commonly at 2.8-5%, is associated with an increased risk of stroke compared to low-grade HAT.[69,71]

Imaging of PDL

Peri-device leak following LAAO presents a notable risk for thromboembolic complications (Table 4). The characteristics of these leaks can vary significantly based on the occlusion device used and the anatomical features of the LAA. With plug-like devices, PDL typically manifests as flow between the left atrium and the distal part of the LAA. With disk-and-lobe devices, PDL may occur between the left atrium and the space between the disk and the lobe or beyond the lobe itself.

The mechanisms of leaks for plug-like devices include edge leak, uncovered lobe or proximal LAA, and fabric leak (Figure 17). For disk-and-lobe devices, leaks can occur between the disk and the lobe, at the distal LAA owing to uncovered proximal tissue, or from fabric

leak.[77] The clinical implications of the different types of leaks with disk-and-lobe devices have not been adequately studied, highlighting the need for further research.

Size of PDLs and Thromboembolic Risk

Traditionally a vena contracta of PDL edge leak of <5 mm has been considered acceptable for the plug-like device; however, emerging data challenge this threshold.[9,72,73,75] Table 3 summarizes key studies showing the PDL incidence and its association with ischemic events. Alkhouli *et al.* reported a 10-15% increase in the 1-year risk-adjusted rates of systemic thromboembolic events for patients with small leaks, with a hazard ratio of 1.152 (95% CI: 1.025-1.294), compared to patients without leaks.[72] Large PDLs, though rare, have been associated with a significantly higher risk of thromboembolism when compared to patients with no PDL.[75] This underscores the importance of accurate detection and ongoing surveillance of these leaks to manage and mitigate associated risks effectively.

Imaging Modalities for Detecting PDL

Detecting and characterizing PDL is critical yet challenging owing to varied detection methods and the lack of a standardized definition. Transesophageal echocardiography and MDCT are the primary imaging modalities used to assess PDL. In a study involving 346 patients who underwent both TEE and MDCT at 8 weeks post-LAAO with a disk-and-lobe device, PDL was detected in 110 patients (32%) via TEE whereas MDCT identified PDL in 210 patients (61%).[78] Another study also demonstrated that the incidence of PDL detected by MDCT was higher (52%) than observed with TEE (34.3%).[79] These studies indicate a substantially higher occurrence of PDL detection with MDCT compared to TEE, revealing a significant discrepancy in leak quantification between these modalities. However, no standardized sizing thresholds currently

exist for cardiac CT, since initial trials were performed with TEE. This highlights an area where further research is needed.

CONCLUSIONS

Multimodality imaging is essential for optimizing outcomes in LAAO. Pre-procedural evaluation using TEE and MDCT is essential for assessing LAA morphology and determining the appropriate device size. Multidetector cardiac computed tomography offers superior multiplanar and 3D imaging, whereas TEE provides functional insights that are vital for determining patient eligibility and selecting the optimal device for the procedure. Intra-procedural imaging with TEE or ICE ensures real-time guidance for accurate and efficient device placement. Post-procedural follow-up with TEE or MDCT is essential for monitoring device stability and assessing PDL and DRT (Central Illustration).

The selection of appropriate imaging modalities for percutaneous LAAO is crucial for ensuring optimal outcomes. The integration of multimodality imaging—leveraging the strengths of TEE, MDCT, and ICE—is essential for accurate device sizing, successful implantation, and timely detection of complications. As imaging technologies advance, these strategies will continue to evolve, further improving long-term outcomes for patients undergoing LAAO.

Acknowledgments

The authors thank Jennifer Pfaff for the editorial preparation of the manuscript and Brian Schurrer for assistance with the figures.

Declarations of Interest

MS is a member of the speaker bureau for Abbott, Boston Scientific, Medtronic, and Philips and the advisory board of Siemens. RJ is a speaker and consultant for Medtronic, Philips, Edwards and GE Healthcare and a member of the advisory board for Medtronic and GE Healthcare.

Funding

This research did not receive any specific grant from funding agencies in the public, commercial, or not-for-profit sectors.

References

1. Jiao M, Liu C, Liu Y, et al. Estimates of the global, regional, and national burden of atrial fibrillation in older adults from 1990 to 2019: insights from the Global Burden of Disease study 2019. Front Public Health 2023;11:1137230.

2. Lin HJ, Wolf PA, Kelly-Hayes M, et al. Stroke severity in atrial fibrillation. The Framingham Study. Stroke 1996;27:1760-4.

3. Blackshear JL, Odell JA. Appendage obliteration to reduce stroke in cardiac surgical patients with atrial fibrillation. Ann Thorac Surg 1996;61:755-9.

4. Holmes DR, Jr., Alkhouli M, Reddy V. Left atrial appendage occlusion for the unmet clinical needs of stroke prevention in nonvalvular atrial fibrillation. Mayo Clin Proc 2019;94:864-74.

5. Madden JL. Resection of the left auricular appendix; a prophylaxis for recurrent arterial emboli. J Am Med Assoc 1949;140:769-72.

6. Reddy VY, Sievert H, Halperin J, et al. Percutaneous left atrial appendage closure vs warfarin for atrial fibrillation: a randomized clinical trial. JAMA 2014;312:1988-98.

7. Holmes DR, Jr., Kar S, Price MJ, et al. Prospective Randomized Evaluation of the Watchman Left Atrial Appendage Closure Device in Patients With Atrial Fibrillation Versus Long-term Warfarin Therapy: the PREVAIL trial. J Am Coll Cardiol 2014;64:1-12.

8. Reddy VY, Doshi SK, Kar S, et al. 5-year outcomes after left atrial appendage closure: from the PREVAIL and PROTECT AF trials. J Am Coll Cardiol 2017;70:2964-75.

9. Lakkireddy D, Thaler D, Ellis CR, et al. Amplatzer Amulet Left Atrial Appendage Occluder versus Watchman device for stroke prophylaxis (Amulet IDE): a randomized, controlled trial. Circulation 2021;144:1543-52.

10. Holmes DR, Reddy VY, Turi ZG, et al. Percutaneous closure of the left atrial appendage versus warfarin therapy for prevention of stroke in patients with atrial fibrillation: a randomised non-inferiority trial. Lancet 2009;374:534-42.

11. Hahn RT, Saric M, Faletra FF, et al. Recommended standards for the performance of transesophageal echocardiographic screening for structural heart intervention: from the American Society of Echocardiography. J Am Soc Echocardiogr 2022;35:1-76.

12. Hayes DE, Bamira D, Vainrib AF, et al. Left atrial appendage tilt-up-and-turn-left maneuver: a novel three-dimensional transesophageal echocardiography imaging maneuver to characterize the left atrial appendage and to improve transcatheter closure guidance. CASE 2023;7:391-5.

13. Vainrib A, Saric M. Quick three-dimensional transesophageal echocardiography of left atrial appendage (LAA) anatomy using the LAA multiview technique. CASE 2023;7:461-2.

14. Zhang L, Cong T, Liu A. Percutaneous closure of the left atrial appendage: the value of real time 3D transesophageal echocardiography and the intraoperative change in the size of the left atrial appendage. Echocardiography 2019;36:537-45.

15. Yosefy C, Laish-Farkash A, Azhibekov Y, et al. A new method for direct three-dimensional measurement of left atrial appendage dimensions during transesophageal echocardiography. Echocardiography 2016;33:69-76.

16. Filby SJ, Dallan LAP, Cochet A, et al. Left atrial appendage occlusion using cardiac CT angiography and intracardiac echocardiography: a prospective, single-center study. J Invasive Cardiol 2021;33:E851-6.

17. Korsholm K, Berti S, Iriart X, et al. Expert recommendations on cardiac computed tomography for planning transcatheter left atrial appendage occlusion. JACC Cardiovasc Interv 2020;13:277-92.

18. Romero J, Husain SA, Kelesidis I, et al. Detection of left atrial appendage thrombus by cardiac computed tomography in patients with atrial fibrillation: a meta-analysis. Circ Cardiovasc Imaging 2013;6:185-94.

19. Hell MM, Achenbach S, Yoo IS, et al. 3D printing for sizing left atrial appendage closure device: head-to-head comparison with computed tomography and transoesophageal echocardiography. EuroIntervention 2017;13:1234-41.

20. Obasare E, Mainigi SK, Morris DL, et al. CT based 3D printing is superior to transesophageal echocardiography for pre-procedure planning in left atrial appendage device closure. Int J Cardiovasc Imaging 2018;34:821-31.

21. Hozman M, Herman D, Zemanek D, et al. Transseptal puncture in left atrial appendage closure guided by 3D printing and multiplanar CT reconstruction. Catheter Cardiovasc Interv 2023;102:1331-40.

22. De Backer O, Iriart X, Kefer J, et al. Impact of computational modeling on transcatheter left atrial appendage closure efficiency and outcomes. JACC Cardiovasc Interv 2023;16:655-66.

23. Wang DD, Eng M, Kupsky D, et al. Application of 3-dimensional computed tomographic image guidance to WATCHMAN implantation and impact on early operator learning curve: single-center experience. JACC Cardiovasc Interv 2016;9:2329-40.

24. Saw J, Fahmy P, Spencer R, et al. Comparing measurements of CT angiography, TEE, and fluoroscopy of the left atrial appendage for percutaneous closure. J Cardiovasc Electrophysiol 2016;27:414-22.

25. Eng MH, Wang DD, Greenbaum AB, et al. Prospective, randomized comparison of 3-dimensional computed tomography guidance versus TEE data for left atrial appendage occlusion (PRO3DLAAO). Catheter Cardiovasc Interv 2018;92:401-7.

26. Sattar Y, Kompella R, Ahmad B, et al. Comparison of left atrial appendage parameters using computed tomography vs. transesophageal echocardiography for watchman device implantation: a systematic review & meta-analysis. Expert Rev Cardiovasc Ther 2022;20:151-60.

27. Ellis CR. Amplatzer Amulet™ left atrial appendage occluder: a step-by-step guide to device implantation. J Cardiovasc Electrophysiol 2022;33:1881-7.

28. Tzikas A, Bergmann MW. Left atrial appendage closure: patient, device and post-procedure drug selection. EuroIntervention 2016;12 Suppl X:48-54.

29. Posada-Martinez EL, Trejo-Paredes C, Ortiz-Leon XA, et al. Differentiating spontaneous echo contrast, sludge, and thrombus in the left atrial appendage: can ultrasound enhancing agents help? Echocardiography 2019;36:1413-7.

30. Porter TR, Mulvagh SL, Abdelmoneim SS, et al. Clinical applications of ultrasonic enhancing agents in echocardiography: 2018 American Society of Echocardiography guidelines update. J Am Soc Echocardiogr 2018;31:241-74.

31. Catino AB, Ross A, Suksaranjit P, et al. Improved thrombus assessment by transesophageal echocardiography: The DOLOP (Detection of Left Atrial Appendage Thrombosis Utilizing Optison) Study. J Am Soc Echocardiogr 2021;34:916-7.

32. Yamashita E, Kemi Y, Sasaki T, et al. Stepwise increase of isoproterenol bolus dose method for differentiating left atrial appendage sludge from thrombus. J Am Soc Echocardiogr 2023;36:553-5.

33. Bhattal GK, Wang Z, Al-Azizi K. Dobutamine-supported WATCHMAN FLX implant in a patient with recurrent left atrial appendage thrombus and spontaneous echo contrast formation. Baylor Univ Med Cent Proc 2022;35:517-9.

34. Pandey AC, Shen CP, Chu E, et al. Inotropes to differentiate dense spontaneous echo contrast from thrombus in the left atrial appendage. JACC Clin Electrophysiol 2023;9:2655-7.

35. Fukutomi M, Fuchs A, Bieliauskas G, et al. Computed tomography-based selection of transseptal puncture site for percutaneous left atrial appendage closure. EuroIntervention 2022;17:e1435-e44.

36. Saw J, Holmes DR, Cavalcante JL, et al. SCAI/HRS expert consensus statement on transcatheter left atrial appendage closure. Heart Rhythm 2023;20:e1-16.

37. Aminian A, Leduc N, Freixa X, et al. Left atrial appendage occlusion under miniaturized transesophageal echocardiographic guidance and conscious sedation: multicenter European experience. JACC Cardiovasc Interv 2023;16:1889-98.

38. MacDonald ST, Newton JD, Ormerod OJ. Intracardiac echocardiography off piste? Closure of the left atrial appendage using ICE and local anesthesia. Catheter Cardiovasc Interv 2011;77:124-7.

39. Berti S, Paradossi U, Meucci F, et al. Periprocedural intracardiac echocardiography for left atrial appendage closure: a dual-center experience. JACC Cardiovasc Interv 2014;7:1036-44.

40. Zhang ZY, Li F, Zhang J, et al. A comparable efficacy and safety between intracardiac echocardiography and transesophageal echocardiography for percutaneous left atrial appendage occlusion. Front Cardiovasc Med 2023;10:1194771.

41. Berti S, Pastormerlo LE, Santoro G, et al. Intracardiac versus transesophageal echocardiographic guidance for left atrial appendage occlusion: The LAAO Italian Multicenter Registry. JACC Cardiovasc Interv 2018;11:1086-92.

42. Flautt T, Da-Wariboko A, Lador A, et al. Left atrial appendage occlusion without fluoroscopy: optimization by 4D intracardiac echocardiography. JACC Cardiovasc Interv 2022;15:1592-4.

43. Chu H, Du X, Shen C, et al. Left atrial appendage closure with zero fluoroscopic exposure via intracardiac echocardiographic guidance. J Formos Med Assoc 2020;119:1586-92.

44. Zahid S, Gowda S, Hashem A, et al. Feasibility and safety of intracardiac echocardiography use in transcatheter left atrial appendage closure procedures. J Soc Cardiovasc Angiogr Interv 2022;1:100510.

45. Berti S, Santoro G, Brscic E, et al. Left atrial appendage closure using AMPLATZER™ devices: a large, multicenter, Italian registry. Int J Cardiol 2017;248:103-7.

46. Boersma LV, Schmidt B, Betts TR, et al. Implant success and safety of left atrial appendage closure with the WATCHMAN device: peri-procedural outcomes from the EWOLUTION registry. Eur Heart J 2016;37:2465-74.

47. Reddy VY, Möbius-Winkler S, Miller MA, et al. Left atrial appendage closure with the Watchman device in patients with a contraindication for oral anticoagulation: the ASAP study (ASA Plavix Feasibility Study With Watchman Left Atrial Appendage Closure Technology). J Am Coll Cardiol 2013;61:2551-6.

48. Landmesser U, Schmidt B, Nielsen-Kudsk JE, et al. Left atrial appendage occlusion with the AMPLATZER Amulet device: periprocedural and early clinical/echocardiographic data from a global prospective observational study. EuroIntervention 2017;13:867-76.

49. Nestelberger T, Alfadhel M, McAlister C, et al. Follow up imaging after left atrial appendage occlusion-something or nothing and for how long? Card Electrophysiol Clin 2023;15:157-68.

50. Alkhouli M, Alarouri H, Kramer A, et al. Device-related thrombus after left atrial appendage occlusion: clinical impact, predictors, classification, and management. JACC Cardiovasc Interv 2023;16:2695-707.

51. Kar S, Doshi SK, Sadhu A, et al. Primary outcome evaluation of a next-generation left atrial appendage closure device: results from the PINNACLE FLX Trial. Circulation 2021;143:1754-62.

52. Sedaghat A, Vij V, Al-Kassou B, et al. Device-related thrombus after left atrial appendage closure: data on thrombus characteristics, treatment strategies, and clinical outcomes from the EUROC-DRT-Registry. Circ Cardiovasc Interv 2021;14:e010195.

53. Alkhouli M, Busu T, Shah K, et al. Incidence and clinical impact of device-related thrombus following percutaneous left atrial appendage occlusion: a meta-analysis. JACC Clin Electrophysiol 2018;4:1629-37.

54. Dukkipati SR, Kar S, Holmes DR, et al. Device-related thrombus after left atrial appendage closure: incidence, predictors, and outcomes. Circulation 2018;138:874-85.

55. Schmidt B, Nielsen-Kudsk JE, Ellis CR, et al. Incidence, predictors, and clinical outcomes of device-related thrombus in the Amulet IDE trial. JACC Clin Electrophysiol 2023;9:96-107.

56. Sedaghat A, Nickenig G, Schrickel JW, et al. Incidence, predictors and outcomes of device-related thrombus after left atrial appendage closure with the WATCHMAN device-insights from the EWOLUTION real world registry. Catheter Cardiovasc Interv 2021;97:E1019-24.

57. Simard T, Jung RG, Lehenbauer K, et al. Predictors of device-related thrombus following percutaneous left atrial appendage occlusion. J Am Coll Cardiol 2021;78:297-313.

58. Fauchier L, Cinaud A, Brigadeau F, et al. Device-related thrombosis after percutaneous left atrial appendage occlusion for atrial fibrillation. J Am Coll Cardiol 2018;71:1528-36.

59. Kaneko H, Neuss M, Weissenborn J, et al. Predictors of thrombus formation after percutaneous left atrial appendage closure using the WATCHMAN device. Heart Vessels 2017;32:1137-43.

60. Aminian A, Schmidt B, Mazzone P, et al. Incidence, characterization, and clinical impact of device-related thrombus following left atrial appendage occlusion in the prospective global AMPLATZER Amulet observational study. JACC Cardiovasc Interv 2019;12:1003-14.

61. Vij V, Piayda K, Nelles D, et al. Clinical and echocardiographic risk factors for device-related thrombus after left atrial appendage closure: an analysis from the multicenter EUROC-DRT registry. Clin Res Cardiol 2022;111:1276-85.

62. Freixa X, Cepas-Guillen P, Flores-Umanzor E, et al. Pulmonary ridge coverage and device-related thrombosis after left atrial appendage occlusion. EuroIntervention 2021;16:e1288-e94.

63. Cepas-Guillén P, Flores-Umanzor E, Leduc N, et al. Impact of device implant depth after left atrial appendage occlusion. JACC Cardiovasc Interv 2023;16:2139-49.

64. Rashid HN, Layland J. Association between device-related thrombus and the neo-appendage with left-atrial appendage occlusion devices. Eur Heart J 2021;42:1047-8.

65. Zhong Z, Gao Y, Kovács S, et al. Impact of left atrial appendage occlusion device position on potential determinants of device-related thrombus: a patient-specific in silico study. Clin Res Cardiol 2024;113:1405-18.

66. Glikson M, Wolff R, Hindricks G, et al. EHRA/EAPCI expert consensus statement on catheter-based left atrial appendage occlusion - an update. Europace 2020;22:184.

67. Main ML, Fan D, Reddy VY, et al. Assessment of device-related thrombus and associated clinical outcomes with the WATCHMAN left atrial appendage closure device for embolic

protection in patients with atrial fibrillation (from the PROTECT-AF trial). Am J Cardiol 2016;117:1127-34.

68. Korsholm K, Jensen JM, Nørgaard BL, et al. Detection of device-related thrombosis following left atrial appendage occlusion: a comparison between cardiac computed tomography and transesophageal echocardiography. Circ Cardiovasc Interv 2019;12:e008112.

69. Kramer AD, Korsholm K, Jensen JM, et al. Cardiac computed tomography following Watchman FLX implantation: device-related thrombus or device healing? Eur Heart J Cardiovasc Imaging 2023;24:250-9.

70. Miller T, Hana D, Patibandla S, et al. Cardiac computed tomography angiography for device-related thrombus assessment after WATCHMAN FLX™ occluder device implantation: a single-center retrospective observational study. Cardiovasc Revasc Med 2022;41:35-46.

71. Iriart X, Blanc G, Bouteiller XP, et al. Clinical implications of CT-detected hypoattenuation thickening on left atrial appendage occlusion devices. Radiology 2023;308:e230462.

72. Alkhouli M, Du C, Killu A, et al. Clinical impact of residual leaks following left atrial appendage occlusion: insights from the NCDR LAAO Registry. JACC Clin Electrophysiol 2022;8:766-78.

73. Reddy VY, Holmes DR Jr., Doshi SK. Peri-device leak after left atrial appendage closure: impact on long-term clinical outcomes (Abstract 16212). Circulation 2021;144:e564-e93.

74. Price MJ, Ellis CR, Nielsen-Kudsk JE, et al. Peridevice leak after transcatheter left atrial appendage occlusion: an analysis of the Amulet IDE trial. JACC Cardiovasc Interv 2022;15:2127-38.

75. Samaras A, Papazoglou AS, Balomenakis C, et al. Residual leaks following percutaneous left atrial appendage occlusion and outcomes: a meta-analysis. Eur Heart J 2024;45:214-29.

76. Hildick-Smith D, Landmesser U, Camm AJ, et al. Left atrial appendage occlusion with the Amplatzer™ Amulet™ device: full results of the prospective global observational study. Eur Heart J 2020;41:2894-901.

77. Alkhouli M, De Backer O, Ellis CR, et al. Peridevice leak after left atrial appendage occlusion: incidence, mechanisms, clinical impact, and management. JACC Cardiovasc Interv 2023;16:627-42.

78. Korsholm K, Jensen JM, Nørgaard BL, et al. Peridevice leak following Amplatzer left atrial appendage occlusion: cardiac computed tomography classification and clinical outcomes. JACC Cardiovasc Interv 2021;14:83-93.

79. Qamar SR, Jalal S, Nicolaou S, et al. Comparison of cardiac computed tomography angiography and transoesophageal echocardiography for device surveillance after left atrial appendage closure. EuroIntervention 2019;15:663-70.

Legends

Figure 1 Commercially approved percutaneous LAAO devices. (A) Plug-like device: This is a self-expanding nitinol device equipped with dual-row precision fixation anchors for enhanced stability. It features a low-profile threaded insert covered by polyethylene terephthalate fabric and is available in 6 sizes, 20-40 mm. (B) Disk-and-lobe device: Composed of a self-expanding nitinol mesh, this device forms a lobe and a disk, connected by a central waist. It is available in 8 sizes, 11-31 mm. *Device images are used with permission from Boston Scientific and Abbott Cardiovascular.*

Figure 2 LAA morphologies illustrated in 2D and 3D TEE. (A) Windsock, (B) chicken wing, (C) cactus, and (D) cauliflower/broccoli LAA morphologies are demonstrated in 2D (left side of each panel) and 3D. 3D TEE utilizes light-source manipulation and transillumination technology to provide high-definition, photorealistic, 3D volume-rendered images of the LAA.

Figure 3 LAAM maneuver to characterize LAA morphology by 3D TEE. (A) Obtain a 3D mid-esophageal LAA en face view at a 2D 45° angle (green line) with the transillumination feature activated. Establish an orthogonal plane (red line) using Multiview. (B) Select the red reference plane and display the cropping plane (dotted lines). (C) Adjust the cropping plane leftward to reveal the full 3D anatomy of the LAA. (D) Rotate the 3D image 90° counterclockwise to simulate the standard fluoroscopic view used during percutaneous LAAO procedures. MV, mitral valve; PA, pulmonary artery.

Figure 4 TUPLE maneuvers to characterize LAA morphology by 3D TEE. (A) Display the standard en face view of the LAA orifice from the left atrial perspective. (B) Apply light-source manipulation to enhance visual details. (C) Utilize transillumination rendering of the LAA, increasing transparency to clearly demonstrate the orifice and outline the walls of the LAA body.

(D) Rotate the image leftward along the vertical axis of the LAA to reveal the full body. (E) Selectively crop tissue to focus on specific areas. (F) Finalize the fully rendered LAA volume after decreasing transparency and increasing image gain. This orientation corresponds to the 2D TEE image at 135º. AV, aortic valve; MV, mitral valve; PA, pulmonary artery.

Figure 5 LAA sizing for LAAO devices. (A) 2D TEE sizing for a plug-like occlusion device. The LAA landing zone diameters and depths are measured at 4 angles: 0º, 45º, 90º, and 135º. The LAA landing zone, which can be up to 2 cm below the left atrial ridge, is depicted by a dotted white line measured at the level of the circumflex artery (red arrow). (B) 2D TEE sizing for the disk-and-lobe device. The LAA landing zone diameters and depths are measured at 4 angles: 0º, 45º, 90º, and 135º. The LAA landing zone diameter is measured 10-12 mm from the anatomic orifice (yellow arrow), and the depth is measured from the ostium to the LAA wall in a plane perpendicular to the ostium. The red arrow indicates the circumflex artery.

Figure 6 Sizing of the LAA orifice using 3D TEE MPR. (A) 3D view of the LAA from the left atrium; the degrees shown correspond to 2D omniplane TEE views to assess the LAA. (B) A single-beat zoom capture acquires the entire LAA and surrounding structures. MPR is obtained. The red and green planes are locked and oriented toward the LAA apex, leaving the blue plane free for adjustment. The blue plane is oriented toward the plane of the LAA orifice, typically at the level of the left circumflex coronary artery (red arrow). The 3D Auto LAA feature (Philips) is used to obtain the maximum diameter of the LAA orifice.

Figure 7 Cardiac computed tomography for pre-procedural planning for LAAO. In addition to excluding LAA thrombi, MDCT with 3D MPR can be utilized to perform precise measurements of the expected landing zone (A), LAA orifice (B), LAA depth, 3D morphology, and relations with the surrounding structures. Advanced software applications can also be of assistance in

planning the optimal transseptal puncture location and C-arm position (C) and display a virtual device in the 3D rendering (D).

Figure 8 Anatomical considerations for LAAO device selection. (A) Favorable morphologies for plug-like LAAO devices include windsock- and cactus-shaped LAAs, typically with orifice diameters ranging from 14-36 mm and depths approximately 50% of the intended device width. Favorable anatomies for disk-and-lobe devices include LAAs with orifice diameters of 11-31 mm and depths of at least 10-12 mm. (B) Unfavorable morphologies for plug-like devices include the chicken wing and cauliflower/broccoli shapes with shallow depths and orifice diameters <14 mm or >36 mm. Unfavorable conditions for disk-and-lobe devices include very small (<11 mm) or very large (>31 mm) landing zone diameters with insufficient depth (<10 mm).

Figure 9 Common steps for LAA closure procedure. (A) Transeptal access. Guided by TEE and fluoroscopy, transseptal access is usually achieved through an inferior and posterior approach. Yellow arrows demonstrate the sheath (Video 1). (B) Guidewire placement. The crossing sheath is exchanged with a guidewire (yellow arrow), which is placed in the LUPV (Video 2). (C) Delivery system advancement. A delivery system with a pigtail catheter (yellow arrow) is advanced into the left atrium. Contrast angiography is performed to fluoroscopically evaluate the LAA (Video 3). (D) Catheter navigation. The guide catheter/pigtail combination is navigated to align the corresponding radiopaque marker band for the device size with the LAA ostium. Once the guide catheter (yellow arrow) is properly positioned, the pigtail is removed. Yellow arrows demonstrate the device and sheath (Video 4).

Figure 10 Plug-like device procedure with TEE. (A) The delivery system (yellow arrow, left panel) is advanced until the distal marker bands of the delivery system and access sheath are

aligned. The device is then unsheathed slowly until a ball shape (yellow arrow, right panel) is visualized (Video 5). (B) The device (yellow arrows) is fully unsheathed, and its position is evaluated using fluoroscopy and TEE (Video 6). (C-E) A pre-release evaluation is conducted using the "PASS" criteria (Position: Ensure that the plane of maximum diameter of the device is at or distal to the LAA ostium. Anchor: Test stability by retracting the deployment knob and letting go, assessing whether the device returns to its original position. Size: Confirm that the device shoulder is compressed to 10-30% of its original size. Seal: Use TEE to assess for any residual flow, which must be <5 mm before release (Video 7). Once all "PASS" criteria are met, the device may be released to deploy (Video 8).

Figure 11 Disk-and-lobe procedure steps with TEE. (A) The cable is advanced to push the device to the tip of the delivery sheath. Subsequently, the sheath is backed out until the device forms the "ball" (yellow arrow). It is essential to verify that the ball is coaxial to the neck of the LAA (Videos 9, 10). (B) The cable is advanced slowly to form the "triangle" shape (yellow arrow) (Video 11). (C) The delivery cable is advanced further to complete the deployment of the device lobe (yellow arrow) (Video 12). (D) Deployment of the device disk (yellow arrow) is completed by advancing the delivery cable while simultaneously unsheathing the device disk (Video 13).

Figure 12 Disk-and-lobe deployment steps with TEE. (A) Once the disk is deployed, a tension test is conducted to ensure the lobe position remains unchanged (Video 14). The yellow arrows point to the football shape of the disk. (B) Residual flow around the device is assessed using TEE (Video 15). (C) After checking for any leaks and verifying a suitable position for release, the "CLOSE" criteria are re-evaluated before the device is released (Video 16). (D) Following deployment, the device is visualized on conventional 3D TEE (Video 17). The red arrow

indicates the proximal end screw. (E) The disk-and-lobe occluder device using light source manipulation, showcasing a figure of 8. Yellow arrows demonstrate the device and sheath.

Figure 13 Assessment of device release PASS criteria for plug-like device. The yellow arrows indicate the threaded insert, the red arrow indicates the left circumflex artery, and the blue double-headed arrow indicates compression of 15%.

Figure 14 Assessment of device release CLOSE criteria for disk-and-lobe device.

Figure 15 Standard ICE views for LAAO. (A) The ICE catheter is visualized in the left atrium on fluoroscopy. The three key ICE probe positions commonly utilized to visualize the LAA during LAAO are the (B) mid left atrial view (equivalent to TEE 45º view), the (C) left superior pulmonary vein view (equivalent to TEE 90º view), and the (D) supramitral view (equivalent to TEE 135º view).

Figure 16 DRT. (A) A thrombus (arrow) on a deeply implanted device is seen on 2D TEE. (B) A thrombus (arrow) on the threaded insert of a device is seen on 2D TEE. (C) A device-related thrombus (arrow) in the neo-appendage created between the device face and the left atrial pulmonary vein/LAA ridge is seen on 3D TEE.

Figure 17 Mechanisms of residual leaks after LAAO with a plug-like occluder. (A) Edge leak seen on TEE. (B) Uncovered lobe seen on CT. (C) Fabric leak seen on TEE.

Central Illustration Utility of multimodality imaging for LAAO.

Table 1 Favorable and unfavorable anatomies for left atrial appendage occlusion

Parameter	Favorable characteristics	Unfavorable characteristics
Plug-like device		
Landing zone	14-36 mm	>36 mm
Depth	~50% of device width	<50% of device width
Morphology	Windsock Cactus	Chicken wing, Cauliflower/broccoli
Landing zone shape/ eccentricity index	Round shape	Elliptical shape ≥1.5 eccentricity index
Pectinates		Large mid cavitary pectinates
Disk-and-lobe device		
Landing zone	11-31 mm	<11 mm or >31 mm
Depth	≥10-12 mm	<10 mm
Morphology	Secondary lobes <1 cm from landing zone Chicken wing with short neck, acute bends	
Landing zone shape/ eccentricity index	Oval landing zone	
Pectinates	Large mid cavitary pectinates	

Table 2 Complications of left atrial appendage procedures[7,10,46-48]

Complications	**Percentage**
Serious pericardial effusion	1.2%-4.8%
Major bleeding	0.6%-1.3%
Ischemic stroke	0.2-0.7%
Device embolization	0.1%-0.6%
Procedure-related death	<0.5%
Total major safety events	3.2%-8.7%

Table 3 Summary of studies reporting DRT incidence, imaging modalities, and association with ischemic events

Study	DRT incidence	Patient factors	Procedural factors	Outcomes
Meta-analysis Alkhouli et al.[53]	• 3.8% (pooled incidence) • Following LAAO <90 days: 42% 90 to 365: 57% >365 days: 1% • No difference in DRT incidence between devices	• No specific consistent predictor was identified	• No specific consistent predictor was identified	Increase in ischemic events (13.5% vs. 4.4%; OR 4.15; 95% CI 2.77-6.22; p<0.001; I^2=0)
Protect AF, PREVAIL, CAP, and CAP2 ad hoc analysis Dukkipati et al.[54]	• 3.74% • 51% of DRT detected by scheduled TEE at 1 year • 62% detected during unscheduled TEE at 1 year	• Permanent AF (OR 2.24; 95% CI 1.19-4.2, p=0.012) • History of TIA/stroke (OR 2.31; 95% CI 1.26-4.25; p=0.007) • Vascular disease (OR 2.06; 95% CI 1.08-3.91; p=0.028)	• LAA diameter (OR 1.06; 95% CI 1.01-1.12; p=0.019 • Lower LVEF (OR 0.96 per 1% increase; 95% CI 0.94-0.99; p=0.009)	Higher rates of ischemic stroke or systemic embolization (adjusted HR 3.9; 95% CI 2.3-6.8; p<0.001)
Amulet IDE Schmidt et al.[55]	• 3.9% through 18 months • Amulet: 82% DRT ≤45 days • Watchman: 73.8% DRT >45 days	• AF (HR 2.44; 95% CI 1.42-4.22; p<0.01) • Female sex (HR 1.65; 95% CI 1.01-2.71; p=0.04) • Older age (HR 1.04; 95% CI 1.01-1.08; p=0.02)		No statistically significant associations between DRT and ischemic stroke or systemic embolization (3.1% vs 2.6% with vs without DRT), although numerically there were more strokes and systemic embolization after DRT vs no-DRT in

				the Watchman arm (5.5% vs 2.5%; HR 2.15; 95% CI 0.50-9.19)
EUROC-DRT registry Sedaghat et al.[52]	• Median of 93 days (IQR 54-161) • 82% detected <6 months • 20% detected >6 months		• Deep implantation	Higher stroke rates in patients with residual DRT vs DRT resolution after 1 year (7.6% vs. 6.5%; p=0.09; mortality 15.0% vs. 1.4%; p=0.01)
EWOLUTION registry Sedaghat et al.[56]	• 4.1% by TEE or CT at a median 54 days (IQR 42-111) • 91.2% of DRT detected <3 months or at first TEE	• Permanent AF (82.4 vs. 64.9%; p<0.01) • Dense SEC (26.5 vs. 11.9%; p=0.03)	• LAA diameter (22.8±3.5 vs. 21.1±3.5 mm; p<0.01)	No difference in rate of ischemic stroke/TIA (DRT 1.7 vs. no-DRT 2.2% per year; p=0.8).
Global DRT registry Simard et al.[57]	• 2.8% • ≤180 days: 64% • >180 days: 36%	• Hypercoagulopathy (OR 17.50; 95% CI 3.39-90.45) • Permanent AF, (OR 1.90; 95% CI 1.22-2.97) • Renal insufficiency (OR 4.02; 95% CI 1.22-13.25)	• Pericardial effusion (OR 13.45; 95% CI 1.46-123.52) • Deep implantation >10 mm from limbus (OR 2.41; 95% CI 1.57-3.69)	Increased rates of ischemic stroke in DRT vs no-DRT patients (16.9% vs. 3.6%; p=0.0001)

Multicenter registry c et al.[58]	• 7.2% per year • 8.3% with TEE and 5.3% with CT • Mean time: 3.1±2.6 months	• Older age (HR 1.07; 95% CI 1.01-1.14; p=0.02) • Prior TIA/stroke (HR 3.68; 95% CI 1.17-11.62; p=0.03)	• No OAC (HR 0.26; 95% CI 0.09-0.77; p=0.02) • APT post-LAAO (HR 0.10; 95% CI 0.01-0.76; p=0.03)	Independent predictor of stroke and TIA (HR 4.39; 95% CI 1.05-18.43; p=0.04)
Single center Kaneko et al.[59]	• 5% DRT • 5.1% at 45-day follow-up	• Higher CHA_2DS_2-VASc score (OR 2.8; 95% CI 1.2-7; p=0.02)	• Deep device implantation (OR 24.7; 95% CI 1.3-458.2; p=0.03)	Not assessed
Prospective global Amulet registry Aminiam et al.[60]	• 1.7% per year • DRT scheduled follow-up TEE in 10 cases, unscheduled TEE 7 cases, and CT 1 patient	• Larger LAA orifice width (HR 1.09, 95% CI 1-1.19; p=0.04)		Greater risk for ischemic stroke/TIA (HR 5.27; 95% CI 1.58-17.55; p=0.007)
EUROC-DRT registry Vij et al.[61]	• 20% patients with DRT • TEE: 88.4% of cases detected • CT: 11.6% of cases detected • Mean of 147±219 days	• Age (OR 1.16; 95% CI 1.07-1.25; p<0.01) • Prior stroke/TIA (OR 3.71; 95% CI 1.19-11.56; p=0.02) • SEC (OR 5.08; 95% CI 1.37-18.84; p=0.02)	• Deep implantation predictive in univariate analysis after PSM	Significant increased risk of stroke with DRT 13.55, compared to no DRT 3.8% within 2 years (HR 4.21; 95% CI 1.88-9.49; p<0.01)

AF, atrial fibrillation; APT, antiplatelet; CI, confidence interval; CT, computed tomography; DRT, device-related thrombus; HR, hazard ratio; IQR, interquartile range; LAA, left atrial appendage; LAAO, LAA occlusion; LVEF, left ventricular ejection fraction; OAC, oral anticoagulation; OR, odds ratio; PSM, propensity score matching; SEC, spontaneous echocardiographic contrast; TEE, transesophageal echocardiography; TIA, transient ischemic attack.

Table 4 Summary of studies reporting PDL incidence, imaging modalities, and association with ischemic events

Study	Device(s)	Study population	Imaging modality	PDL incidence	Association of PDL with ischemic events
NCDR LAAO registry[72]	Watchman 2.5	51,333	TEE (45 days)	<5 mm: 25.8% >5 mm: 0.7%	Small PDLs (1-5 mm): ↑ stroke/TIA/systemic embolization (aHR 1.15; 95% CI 1.02-1.29) compared to no PDL
PROTECT AF & PREVAIL+CAP2[73]	Watchman 2.5	1,054	TEE (45 days, 12 months)	≤3 mm: 24.2% 3-5 mm: 14.1% >5 mm: 1.5%	PDL ≤5 mm at 1 year was a significant predictor of ischemic stroke/systemic embolism (HR 1.75; 95% CI 1.06-2.89; p=0.03)
AMULET IDE[9]	Amulet and Watchman 2.5	1,878	TEE (45 days, 12 months)	At 45 days Amulet 0-3 mm: 27% >3-5 mm: 9% >5 mm: 1% Watchman 0-3 mm: 29%, 3-5 mm: 22% >5 mm: 3%	Not assessed
AMULET IDE Sub-analysis[74]	Amulet (801 patients) and Watchman 2.5 (792 patients)	1,593	TEE at 45 days, 12 months	At 45 days Watchman 0-3 mm: 74.1% ≥3-5 mm: 25.9% >5 mm: 3.2% Amulet 0-<3mm: 88.8%	PDL ≥3 mm: higher 1-month rates of ischemic stroke or systemic embolization compared with those with PDL <3 mm (3.6% vs 1.8%; unadjusted HR 2.03; 95% CI 0.96-4.29; p=0.06)

				≥3-5mm: 1.2% >5 mm: 1.1% p<0.01 for all At 12 months Watchman – residual PDL ≤5 mm: 97.2% <5 mm: 2.8% Watchman – new PDL ≥3 mm: 8.3% Amulet – residual PDL ≤5 mm: 99.4% >5 mm: 0.6% Amulet – new PDL ≥ 3mm: 4.2%	
Meta-analysis of residual leaks following LAAO[75]	Amulet and Watchman	61,666	TEE, CT	TEE Any PDL: 26.5% >1 mm: 15% >3 mm: 9.6% >5 mm: 0.9% CT PDL >0 mm: 57.3%	Any TEE-reported PDL was significantly associated with 2-fold increase odds of thromboembolism (pOR 2.04, 95% CI 1.52-2.74; I^2=28%) compared to no PDL
PINNACLE FLX[51]	Watchman FLX	400 patients	TEE (45 days, 6 months, and 1 year)	17.2% at 45 days 10.5% at 6 months (>0 and ≤5 mm) No PDL >5 mm	Not assessed
EWOLUTION[56]	Watchman	835	TEE (45 days)	8.4% (any PDL)	Not assessed

Global Amulet Study[76]	Amulet	1,088	TEE (45 days)	9.9% (any PDL)	Not assessed

aHR, adjusted hazard ratio; CI, confidence interval; CT, computed tomography; HR, hazard ratio; LAAO, left atrial appendage occlusion; OR, odds ratio; pOR, pooled odds ratio; PDL, peri-device leak; TEE, transesophageal echocardiography; TIA, transient ischemic attack.

Video Legends

Video 1 Common steps – transseptal wire on 2D transesophageal echocardiography

Video 2 Common steps – wire in the left upper pulmonary vein on 2D transesophageal echocardiography

Video 3 Common steps – pigtail placement in the left atrial appendage on 2D transesophageal echocardiography

Video 4 Common steps – sheath guided into the left atrial appendage on 3D biplane transesophageal echocardiography

Video 5 Plug-like device – "ball" shape visualized on 3D biplane transesophageal echocardiography

Video 6 Plug-like device – deployed device on 3D biplane on 2D transesophageal echocardiography

Video 7 Plug-like device – deployed device assessed with color Doppler to evaluate for peri-device leak on 2D transesophageal echocardiography

Video 8 Plug-like device – released device in the left atrial appendage on 3D transesophageal echocardiography

Video 9 Disk-and-lobe device – "ball" shape visualized on 3D biplane transesophageal echocardiography

Video 10 Disk-and-lobe device – "ball" shape visualized on 3D transesophageal echocardiography

Video 11 Disk-and-lobe device – "triangle" shape visualized on 3D biplane transesophageal echocardiography

Video 12 Disk-and-lobe device – lobe deployment visualized on 3D biplane transesophageal echocardiography

Video 13 Disk-and-lobe device – disk release is visualized on 3D biplane transesophageal echocardiography

Video 14 Disk-and-lobe device – tension test performed on 3D biplane transesophageal echocardiography

Video 15 Disk-and-lobe device – deployed device assessed with color Doppler to evaluate for peri-device leak on 2D transesophageal echocardiography

Video 16 Disk-and-lobe device – device release visualized on 3D biplane transesophageal echocardiography

Video 17 Disk-and-lobe device – disk released and seen on 3D transesophageal echocardiography

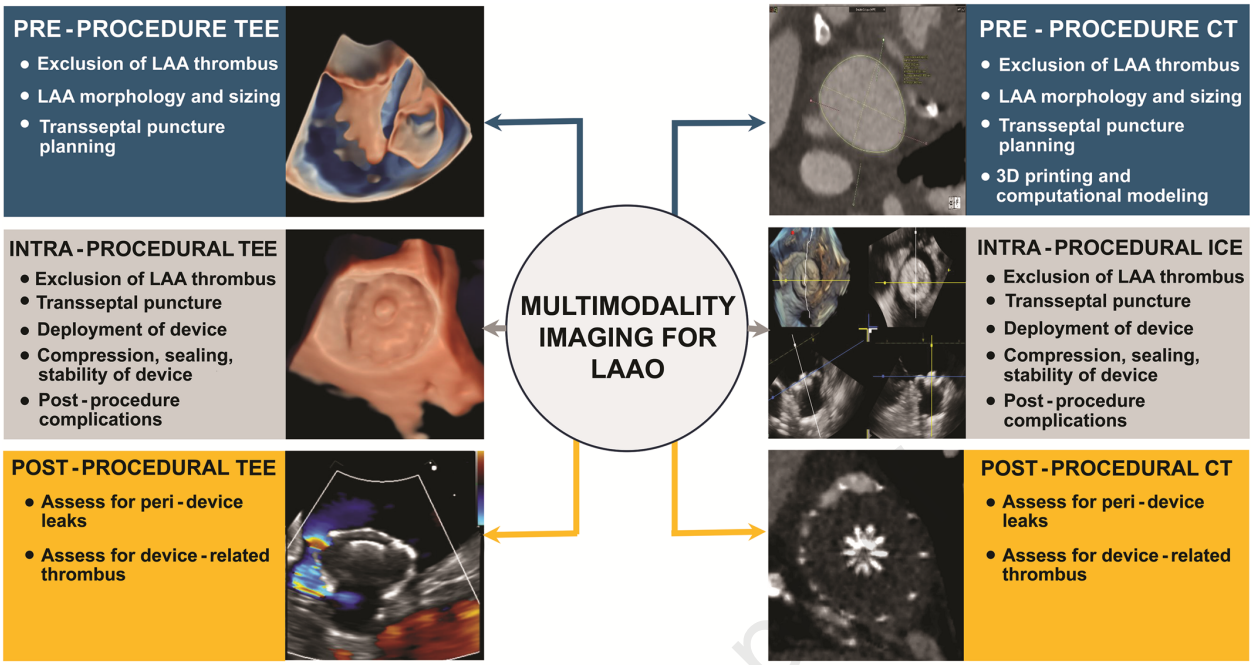

Jain: J Am Soc Echocardiogr 2025

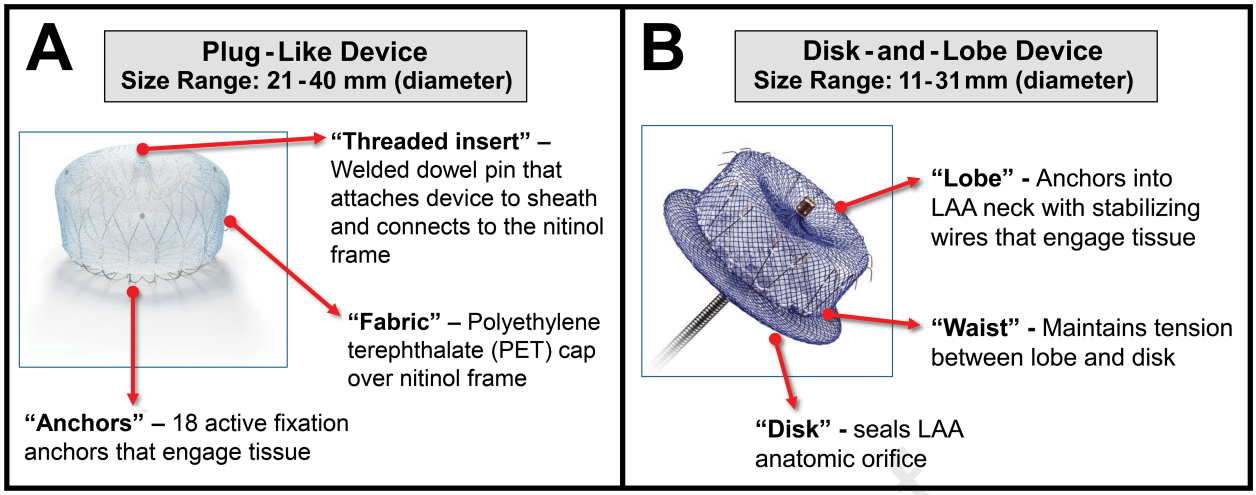

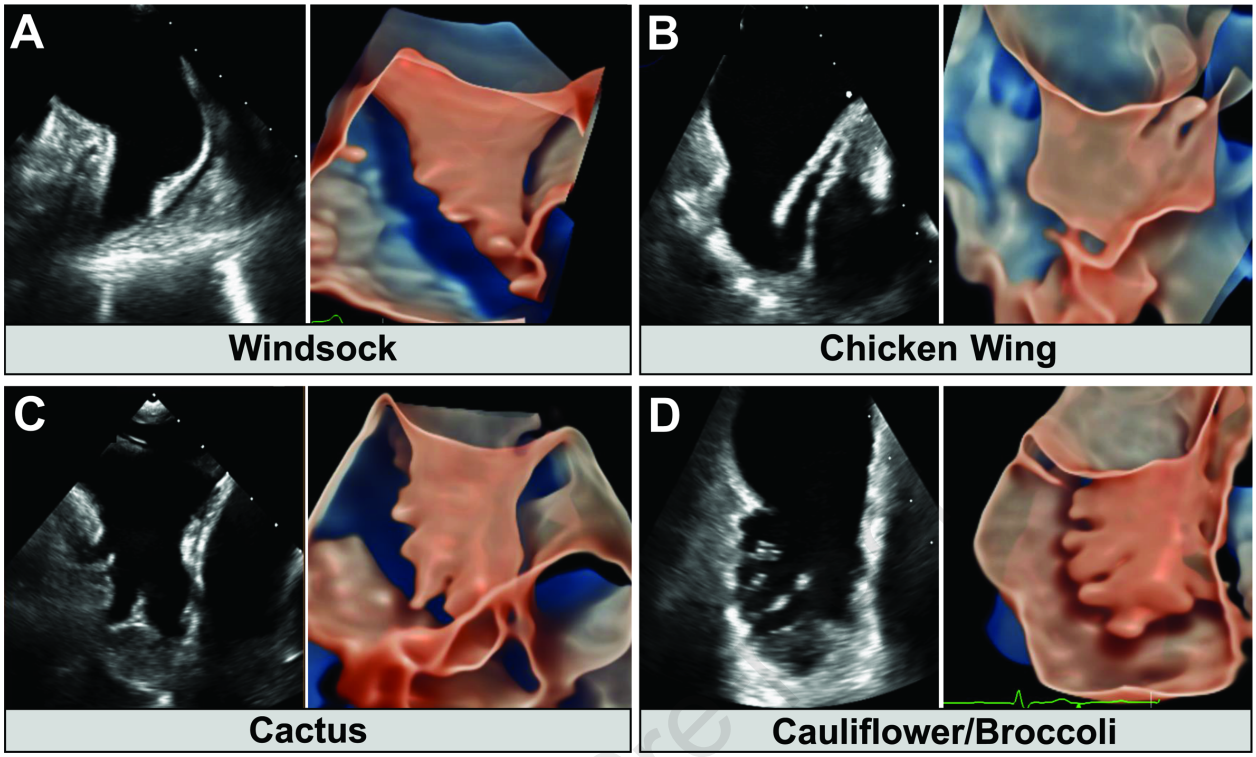

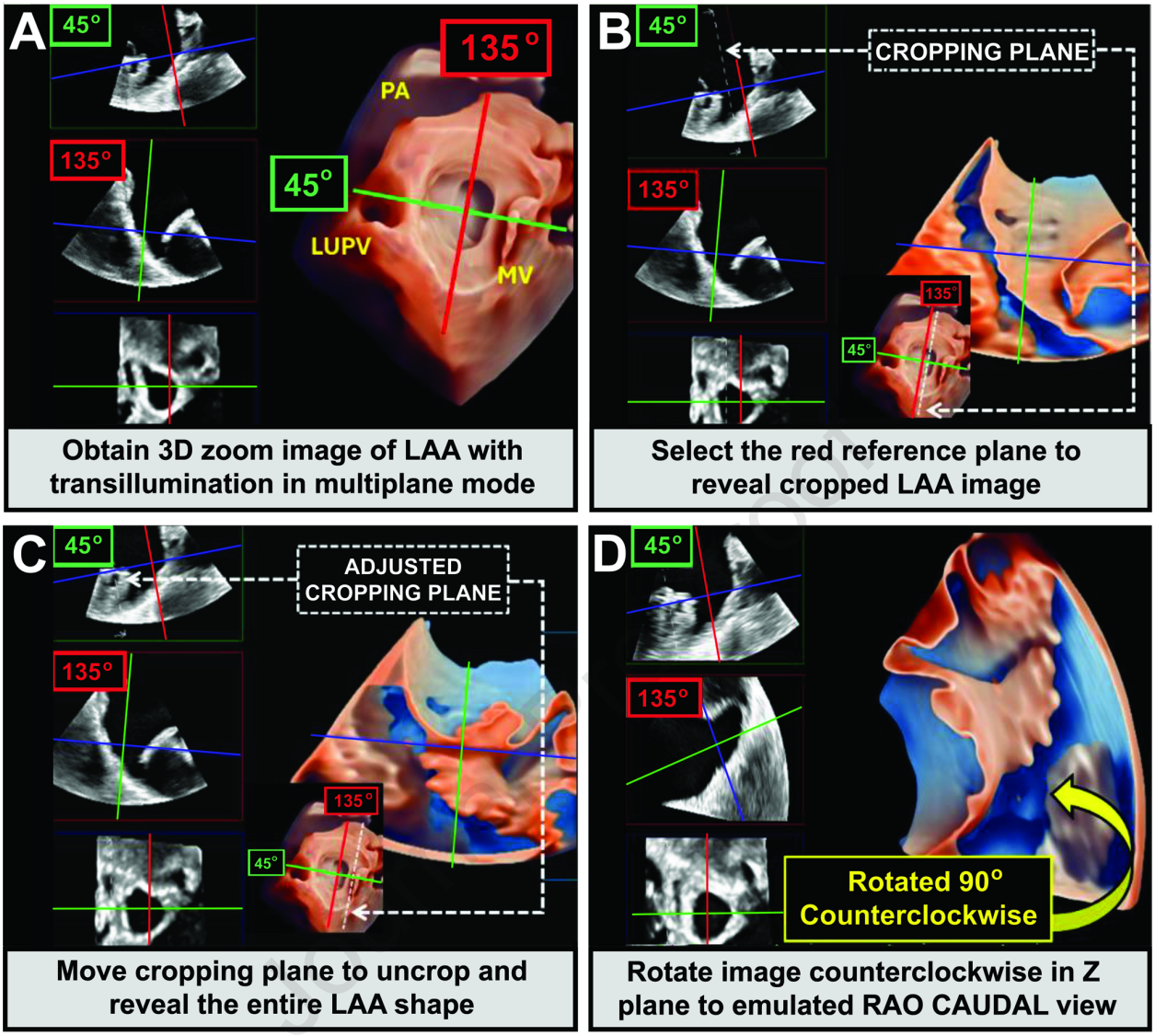
A
45°
135°
135°
45°
PA
LUPV
MV
Obtain 3D zoom image of LAA with transillumination in multiplane mode
B
45°
CROPPING PLANE
135°
135°
45°
Select the red reference plane to reveal cropped LAA image
C
45°
ADJUSTED CROPPING PLANE
135°
135°
45°
Move cropping plane to uncrop and reveal the entire LAA shape
D
45°
135°
Rotated 90° Counterclockwise
Rotate image counterclockwise in Z plane to emulated RAO CAUDAL view

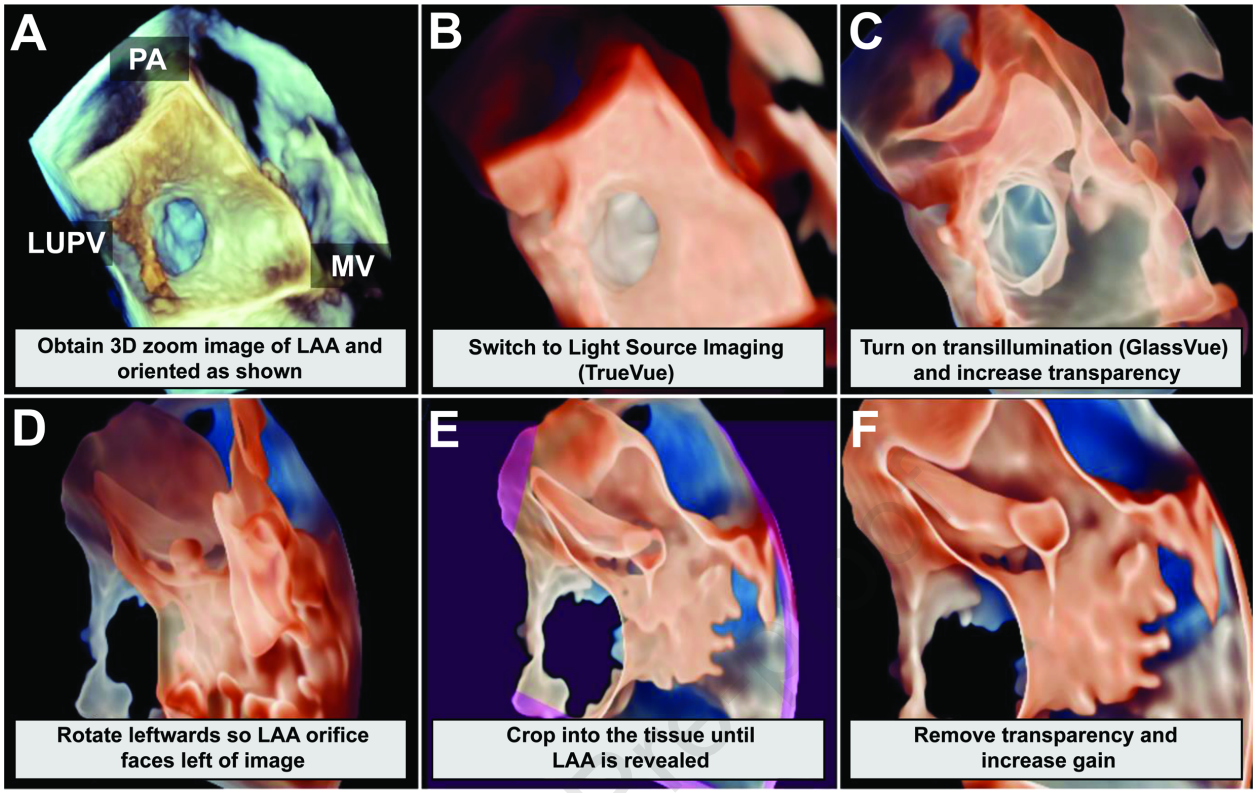

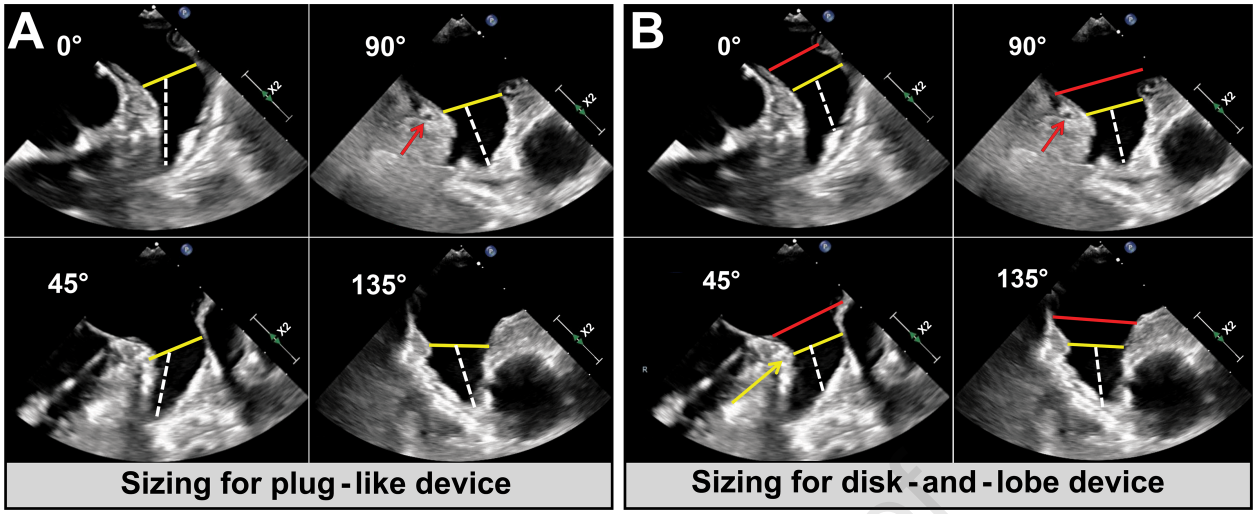

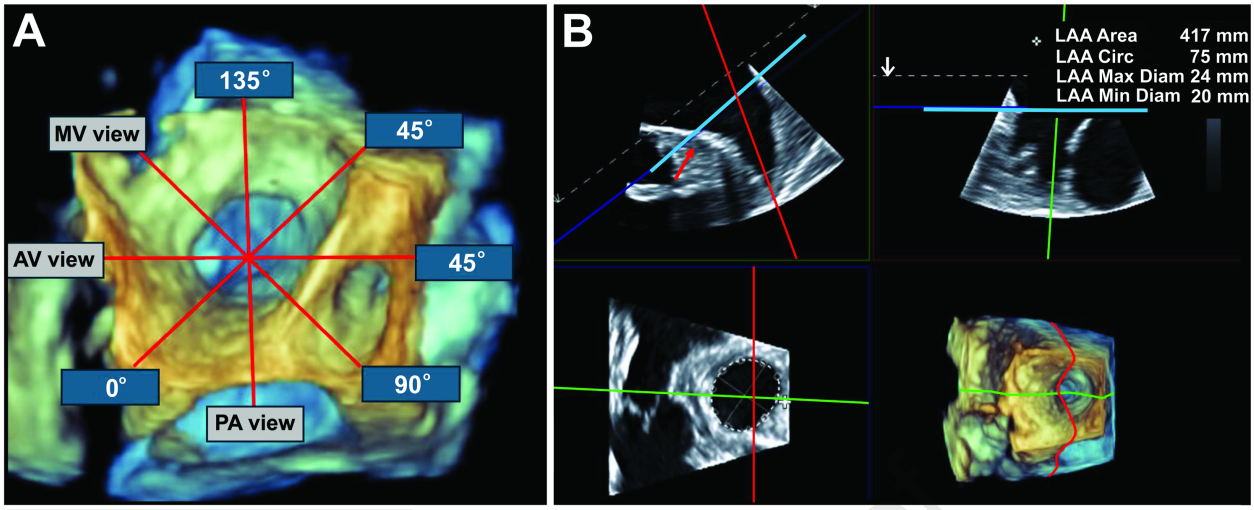

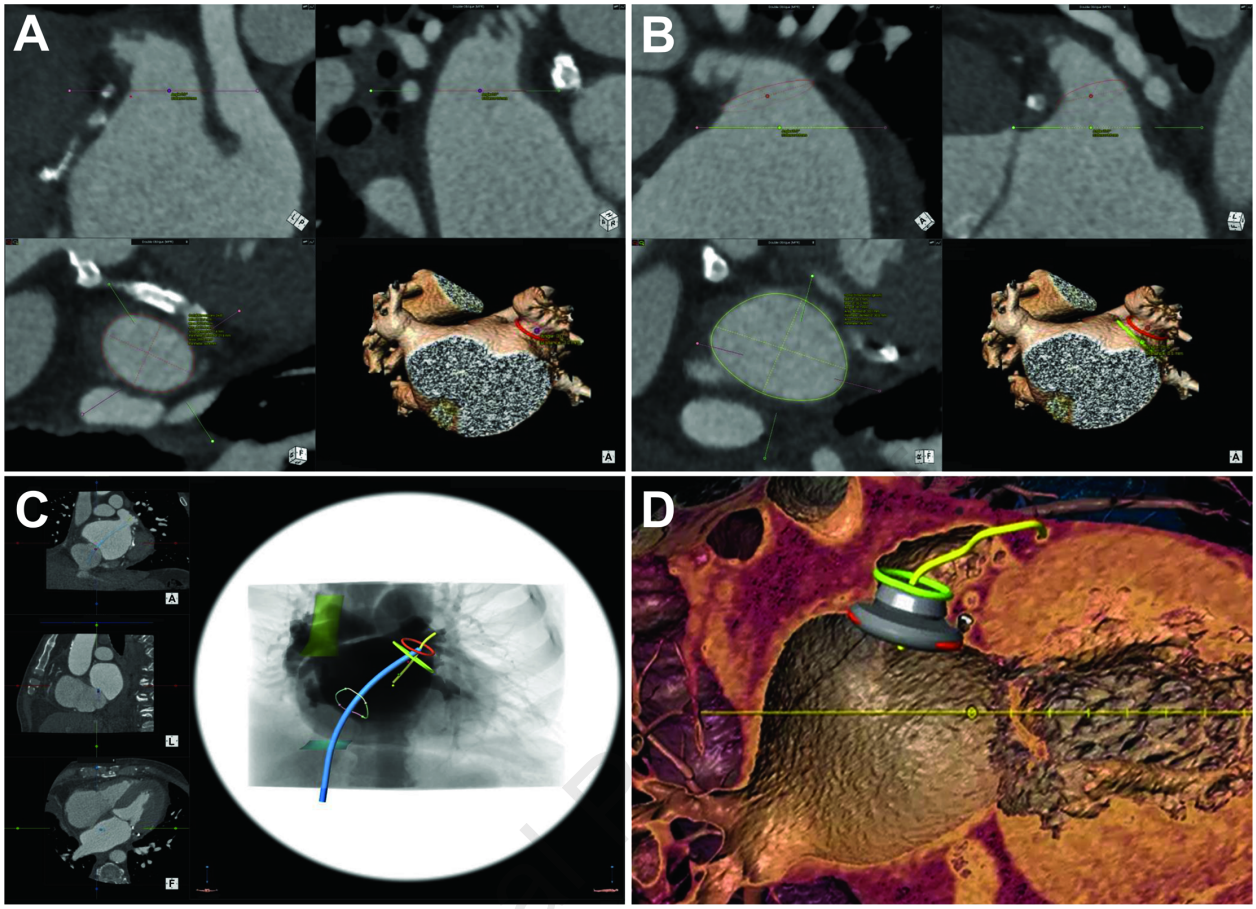

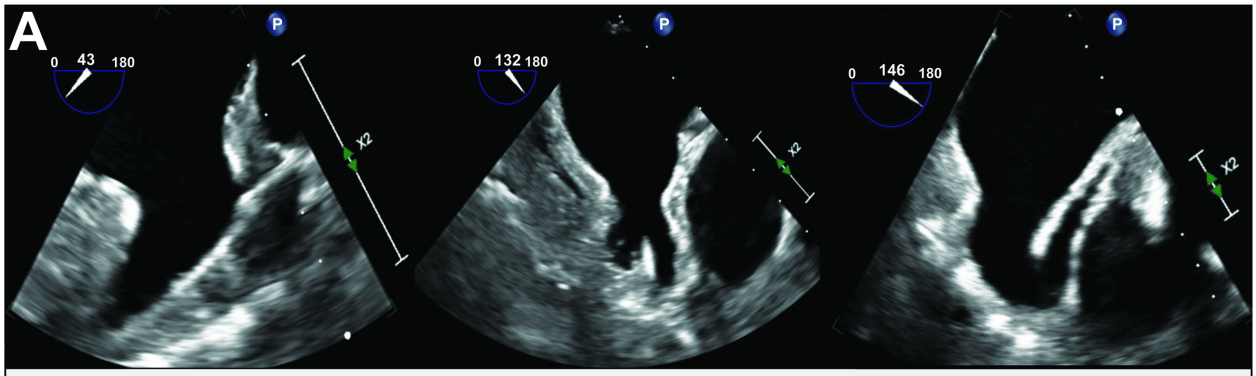

Favorable Anatomies for LAAO

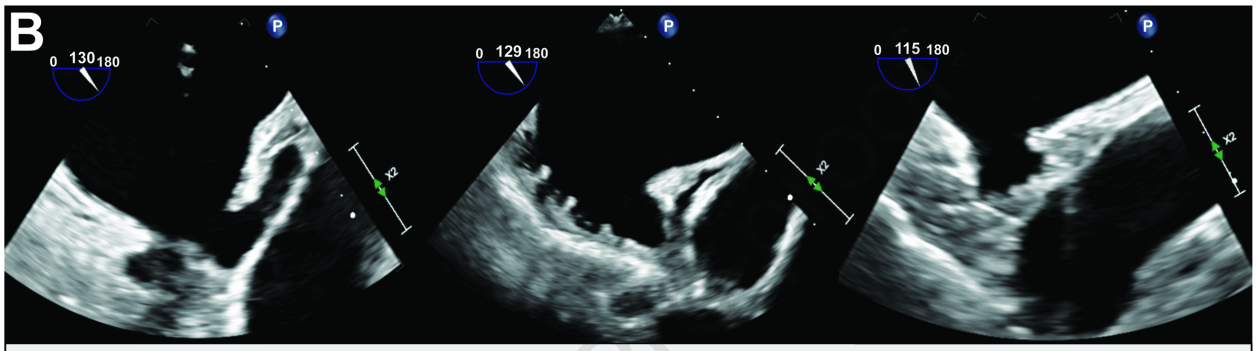

Unfavorable Anatomies for LAAO

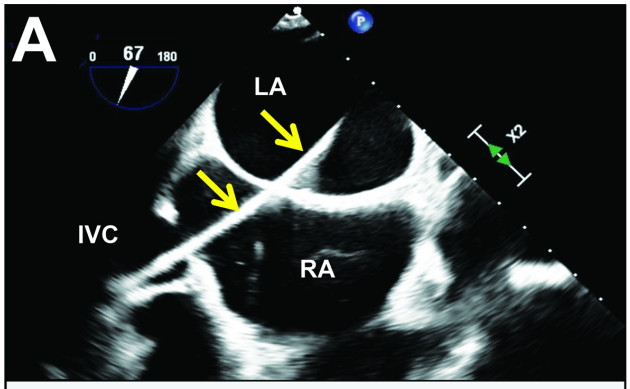

Transseptal Access

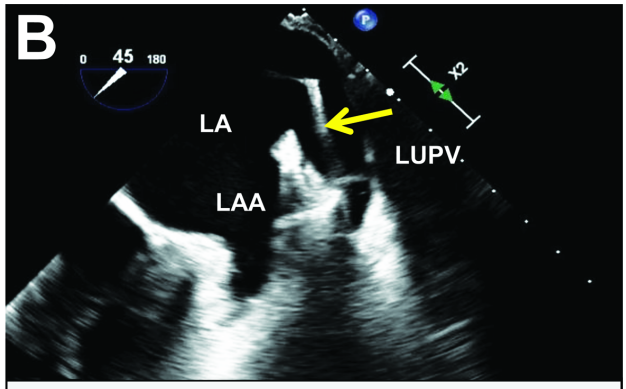

Wire in LUPV

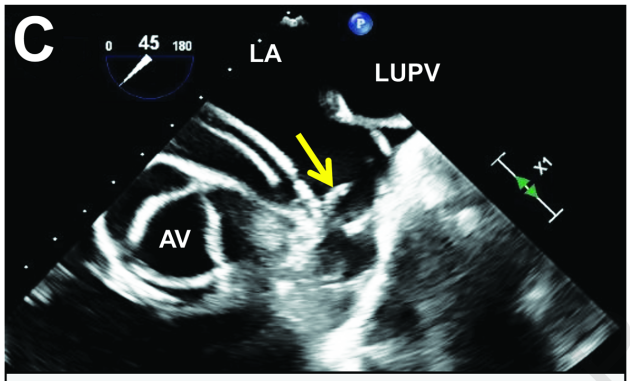

Pigtail in LAA

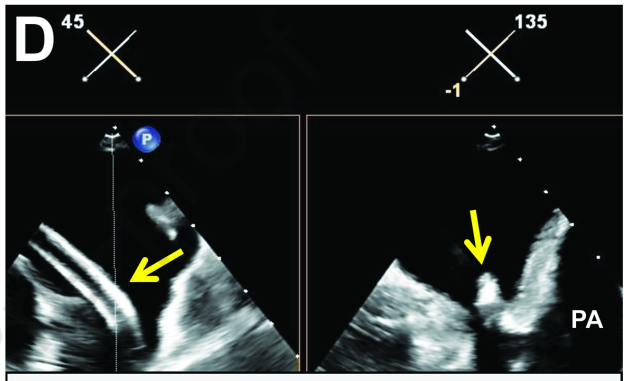

Guide (Delivery Sheath) in LAA

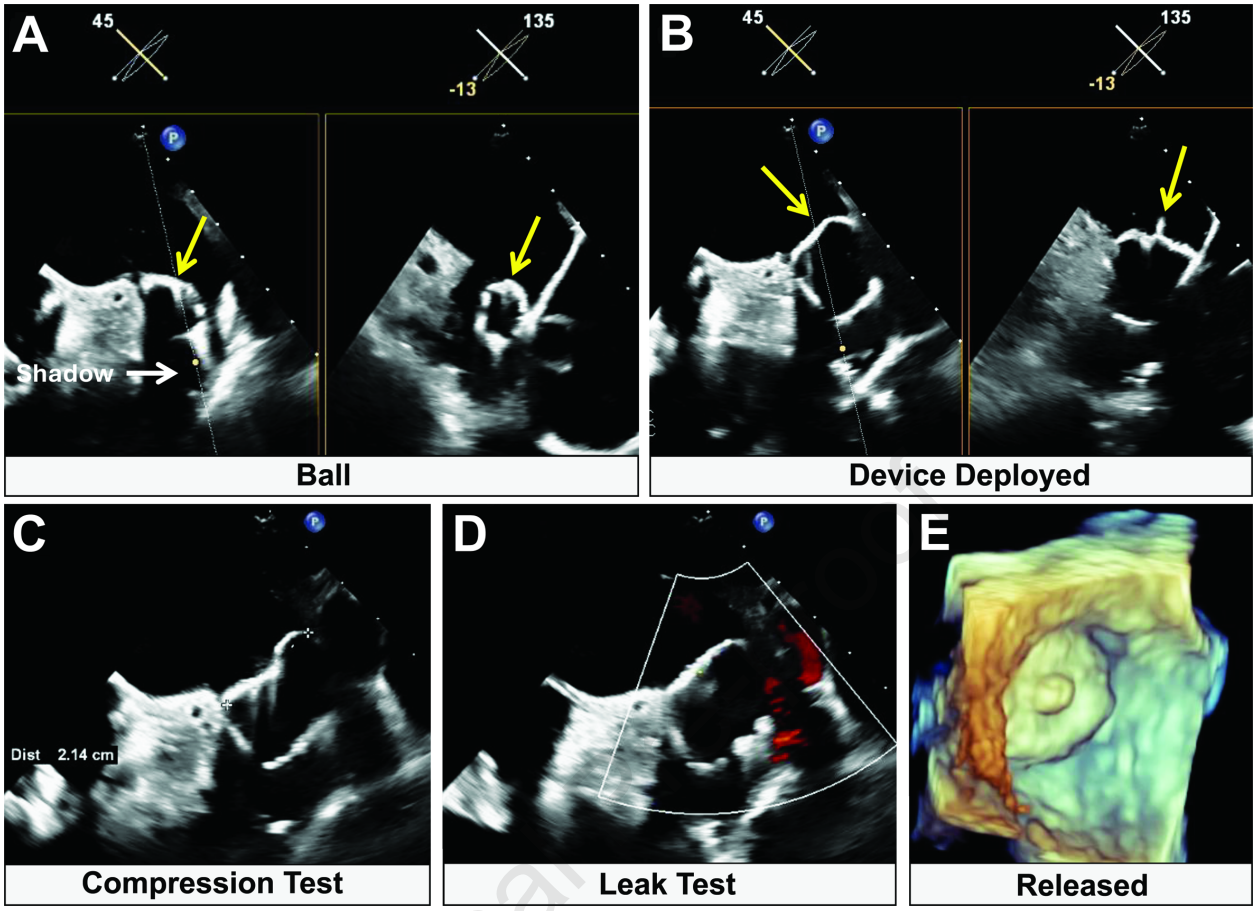

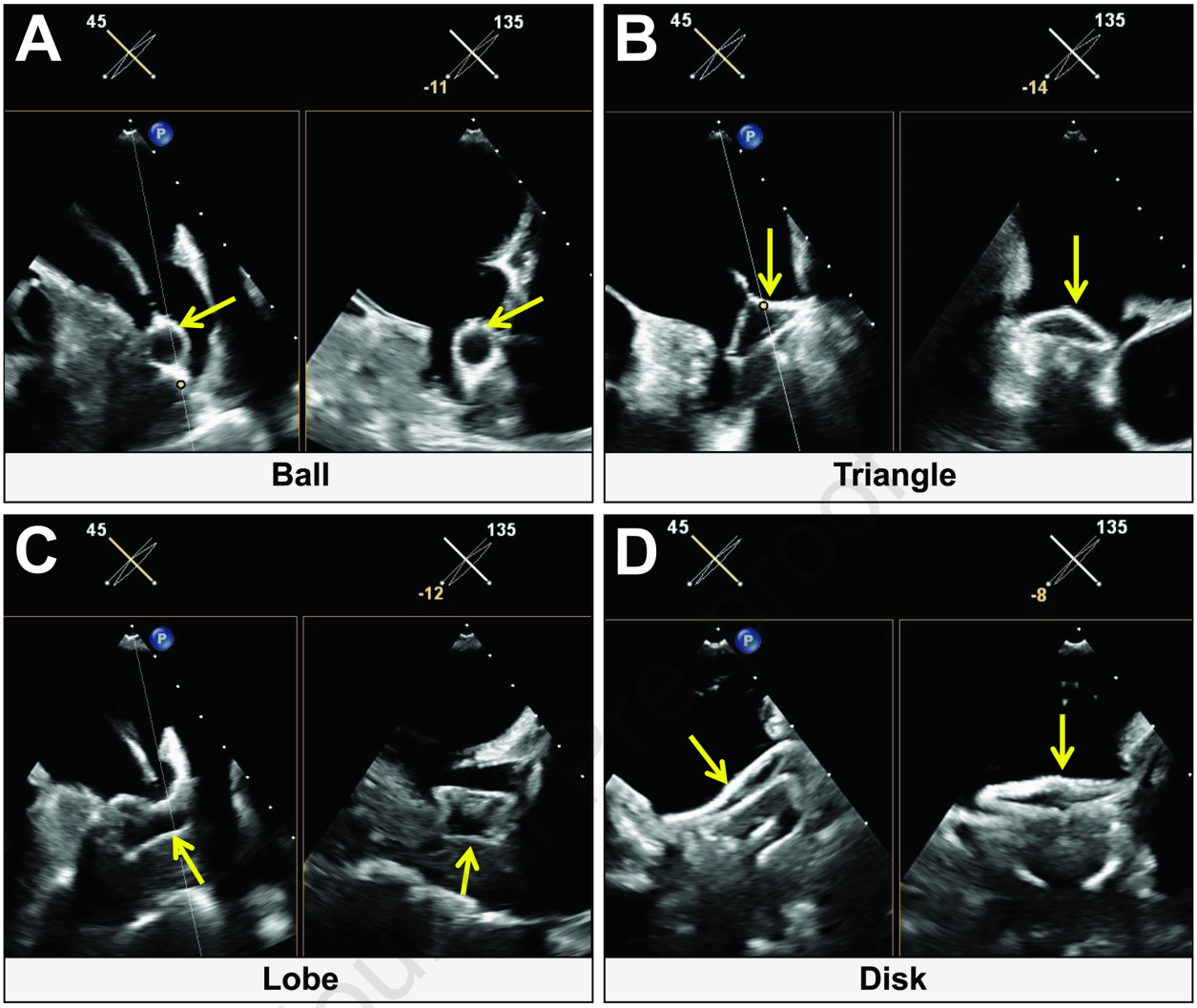
A
45
135
-11
Ball
B
45
135
-14
Triangle
C
45
135
-12
Lobe
D
45
135
-8
Disk

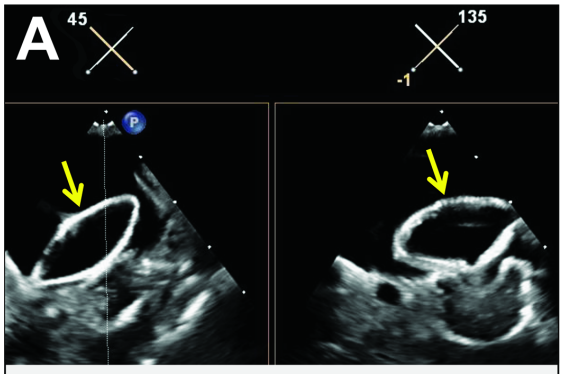

Tension Test

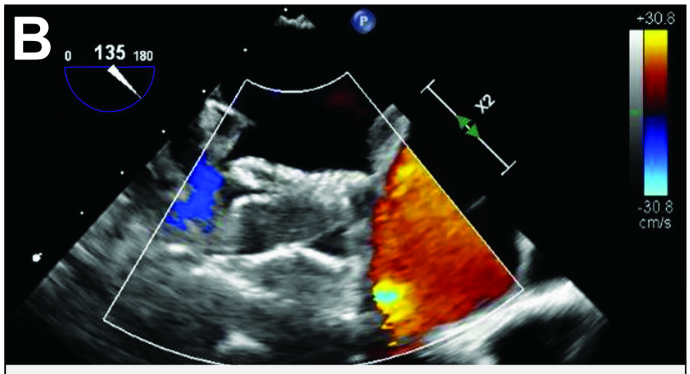

Leak Test

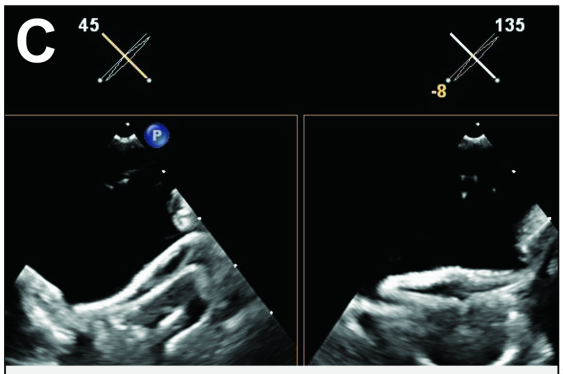

Device Deployed

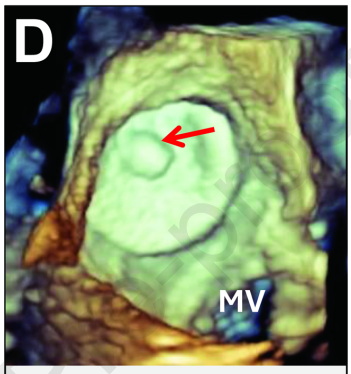

Disk View

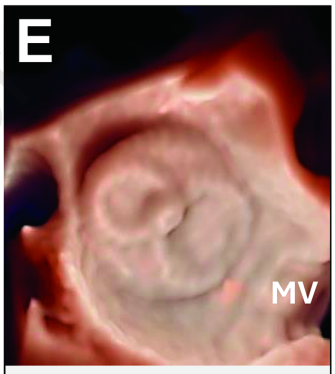

Figure of 8

Position (P)

Device shoulder (white dotted line) at the LAA ostium, or at least two-thirds of the device within the LAA

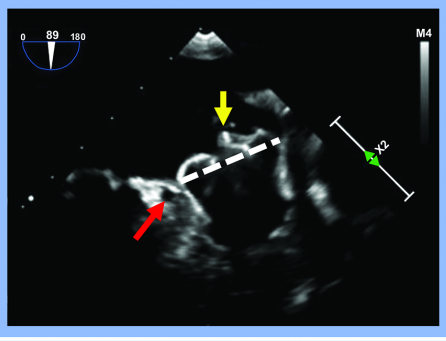

Anchor/Stability (A)

Tug test for stability performed by retracting the deployment knob and letting go, to assess return to original position

Size/Compression (S)

10-30% of the original size compression for appropriate stability

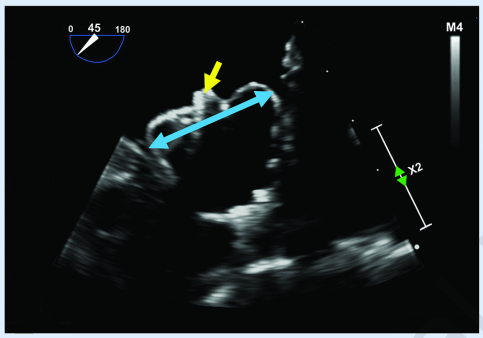

Seal (S)

Ensure all lobes are distal to device and sealed with ≤5 mm PDL on Doppler

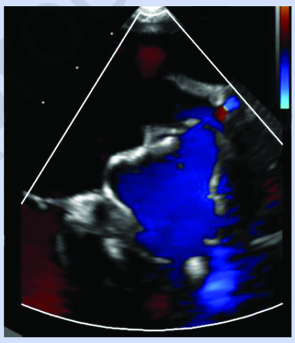

Circumflex (C)
At least two-thirds of the device lobe (yellow arrow) should be distal to the circumflex artery (red arrow)

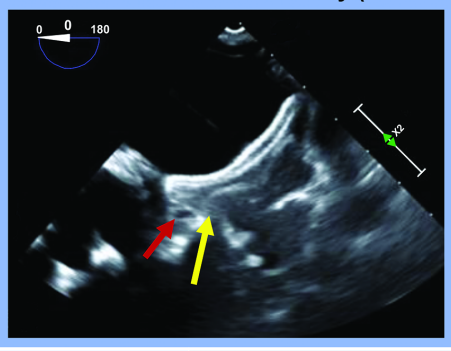

Lobe position (L)
Device lobe should be slightly compressed (tire-shaped) and have good apposition to the LAA wall

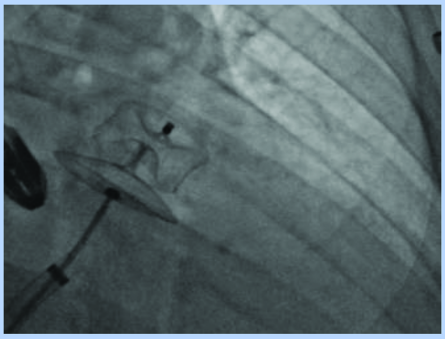

Orientation (O)
Lobe should be coaxial with the landing zone

Separation (S)
The disk (green arrow) must be separated from the lobe (yellow arrow)

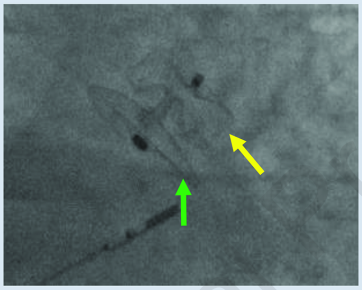

Elliptical (E)
The disk (green arrow) should be a concave shape with respect to the left atrium

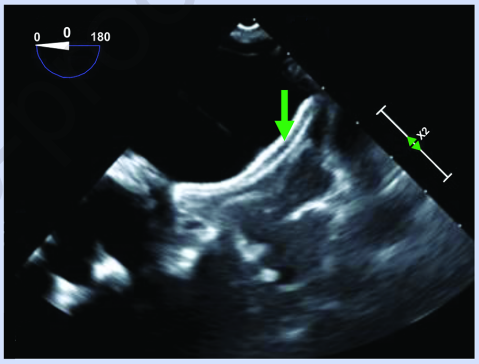

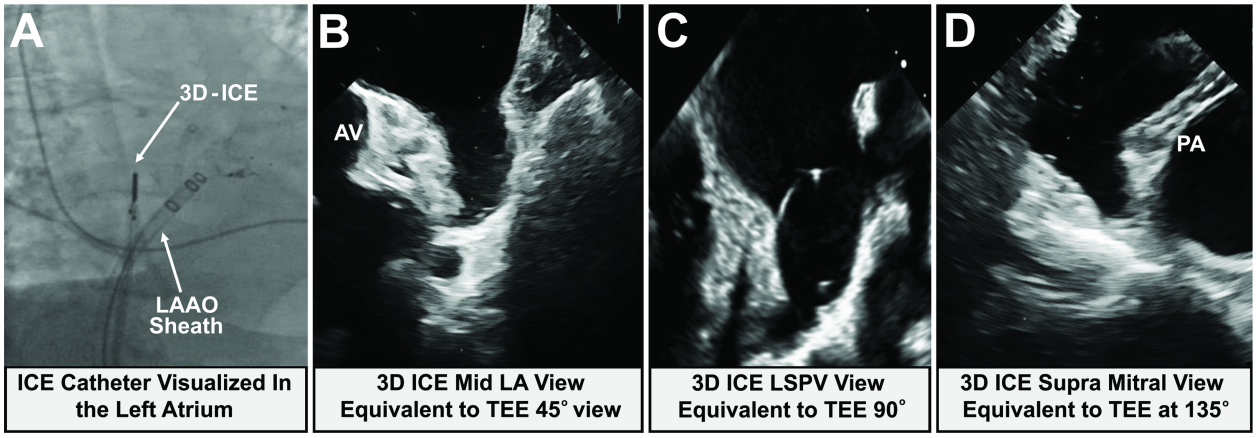

ICE Catheter Visualized In the Left Atrium

3D ICE Mid LA View Equivalent to TEE 45° view

3D ICE LSPV View Equivalent to TEE 90°

3D ICE Supra Mitral View Equivalent to TEE at 135°

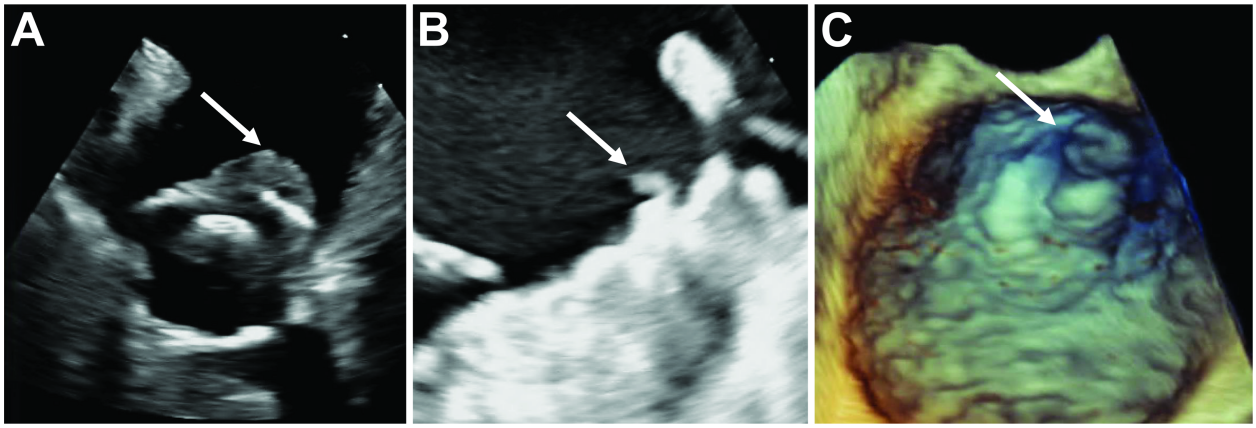

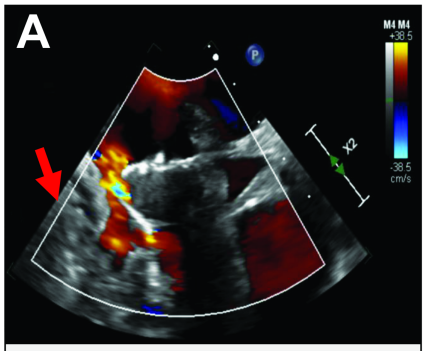

Edge Leak on TEE

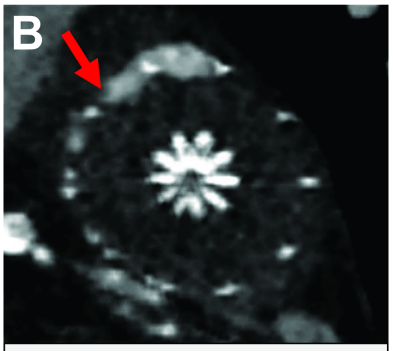

Edge Leak on CT

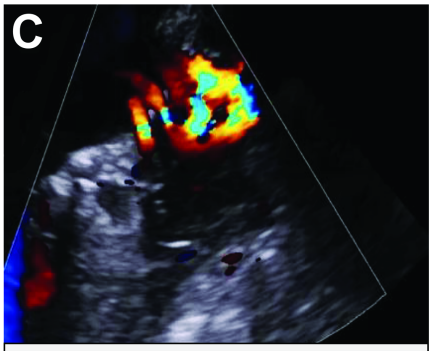

Fabric Leak on TEE

Highlights

- Advanced imaging technologies and techniques have revolutionized LAA occlusion.
- 3D TEE and multiplanar reconstruction aid device sizing and procedural planning.
- MDCT allows 3D printing and virtual device simulation useful during planning.
- 3D ICE can guide transseptal puncture and device deployment.
- Post-procedure, TEE and MDCT can assess device stability and complications.